

# On-chip topological nanophotonic devices



Cui-Cui Lu<sup>1,†,\*</sup> , Hong-Yi Yuan<sup>1,†</sup> , Hong-Yu Zhang<sup>1,†</sup> , Wen Zhao<sup>1</sup>, Nian-En Zhang<sup>1</sup>, Yan-Ji Zheng<sup>1</sup>, Sayed Elshahat<sup>1</sup> & Yong-Chun Liu<sup>2</sup>

<sup>1</sup>Key Laboratory of Advanced Optoelectronic Quantum Architecture and Measurements of Ministry of Education, Beijing Key Laboratory of Nanophotonics and Ultrafine Optoelectronic Systems, School of Physics, Beijing Institute of Technology, Beijing 100081, China <sup>2</sup>State Key Laboratory of Low-Dimensional Quantum Physics, Department of Physics, Frontier Science Center for Quantum Information, Tsinghua University, Beijing 100084, China

<sup>†</sup>These authors contributed equally to this work.

E-mail: cuicuiliu@bit.edu.cn (Cui-Cui Lu)

Cite as: Lu, C.-C. et al. On-chip topological nanophotonic devices. *Chip* 1, 100025 (2022).

<https://doi.org/10.1016/j.chip.2022.100025>

Received: 15 July 2022

Accepted: 21 September 2022

Published online: 28 September 2022

**On-chip topological nanophotonic devices, which take photons as information carriers with topological protection during light propagation, have great application potential in the next generation photonic chips. The topological photonic states enable the nanophotonic devices to be robust and stable, immune to scattering even with imperfect structures. The development, opportunities and challenges of the on-chip topological nanophotonic devices have attracted great attention of scholars, and desired to be known. In this review, topological devices were introduced in the order of functionalities on an integrated photonic chip, i.e. topological light source, topological light waveguiding, topological light division and selection, topological light manipulation and topological light detecting. Finally, we gave outlooks for predicting and promoting the performances of on-chip topological nanophotonic devices from the angles of non-Hermitian systems, non-Abelian topology, metasurfaces, intelligent algorithms and multiple functional topological nanophotonic integration. This review provides rich knowledge about on-chip topological nanophotonic devices. The insights in this paper will spark inspiration and inspire new thinking for the realization of topological photonic chips.**

**Keywords:** Topological photonics, Nanophotonic devices, Photonic chip

## 1. INTRODUCTION

Topology, as a branch of mathematics, was introduced into condensed matter physics by Thouless et al.<sup>1</sup> and Kohmoto<sup>2</sup> when explaining the experiment of quantum Hall effect conducted successfully by K. Klitzing<sup>3</sup>. In recent years, topology has been extended to photonic systems and has achieved great progress<sup>4–6</sup>. The introduction of topology in the photonic realm initially originated from the direct analogy to quantum Hall effect in electronic system where the topology structures of energy bands were described by topological invariants like Chern number.

The analogy of topological photonics was first proposed by Haldane and Raghu<sup>7</sup>. Subsequently, Wang et al. realized a one-way topological waveguide, and the device was achieved in microwave range and immune to large scatters<sup>8,9</sup>, which were early works in the field of topological photonics. After that, motivated by the novel phenomena and rich physics, topological photonics became more and more popular in the research community. Several reviews about topological photonics have been published since 2014<sup>4–6,10–18</sup>. A variety of mechanisms to achieve topological photonic states have been proposed<sup>6</sup>. Topological photonic devices can be designed based on these topological protection mechanisms. For example, one-way waveguides are designed based on the one-way transmission of topological edge states, in which light can propagate with ignorance of defects<sup>19,20</sup>.

In the tide of big data, the development of electronic chips that follow Moore's Law faces great challenges, i.e. increasing heat dissipation and tunneling effect problems<sup>21</sup>. On-chip nanophotonic devices, which carry and process information with photons in the nanoscale, have the advantages of low energy cost and broad bandwidth and are considered potential candidates for the solution in certain application situations, including all-optical connection, all-optical computing, and all-optical network<sup>22–25</sup>. However, there also exist inevitable errors, especially during the preparation process of nano-devices, usually leading to the decay of the functionality. The introduction of topology photonics promises a broad prospect for robust on-chip light information processing. The trend of applying topological states to constructing on-chip nanophotonic devices is growing fast. A number of on-chip topological nanophotonic devices are designed<sup>11,26,27</sup>. Empowered by the robustness of topological edge states, the unbeneficial effects brought by fabrication errors will be suppressed. Noticing the obvious advantages of topological photonics and the importance of on-chip light processing, here we present a review of the on-chip topological nanophotonic devices. As shown in Fig. 1, the introduced devices in our review are divided into six categories according to their respective function, which begins with the topological light source, followed by topological light waveguiding, topological light division and selection, topological light information processing, topological quantum information processing and topological light amplifiers and sensors.

Nine sections are included in the review. The first section is the introduction, where the development of topological photonics and the advantages of topological nanophotonic devices were introduced respectively. The second section is topological light sources, which includes topological lasers and topological quantum light sources. Several typical topological lasers based on different topological systems were firstly summarized in this section, and subsequently introducing the recent development of topological quantum light sources based on ring-resonator systems. In the third section, some typical achievements of topological photonic waveguides were introduced, including the photonic quantum Hall effect, photonic quantum spin Hall effect, photonic Valley Hall effect and topological photonic waveguides arrays. The fourth section is focused on topological

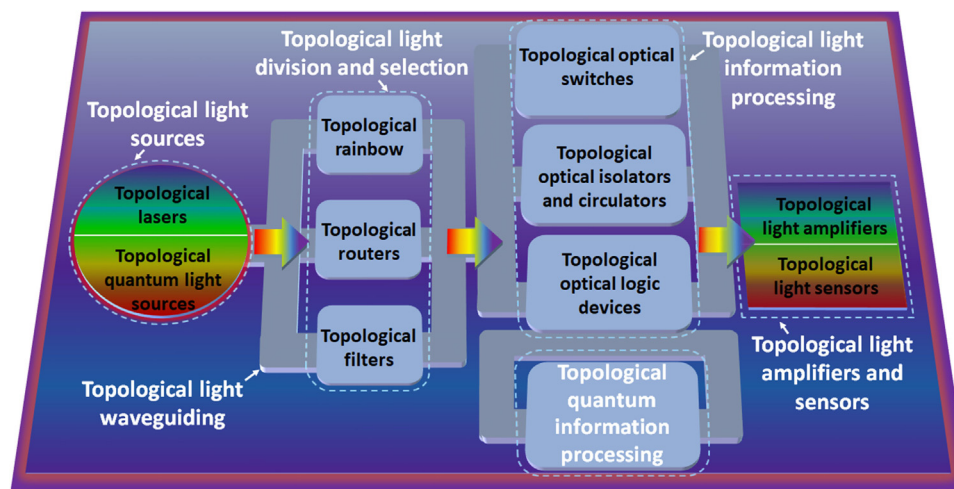


Fig. 1 | The organization of the on-chip topological nanophotonic devices.

light division and selection, introducing the topological rainbow, topological routers, topological power splitter and topological filters, which are key components of photonic chip. The fifth section is the topological light information processing, including topological optical switches, topological optical isolators and circulators, as well as topological optical logic devices which are important devices for manipulation of light signals. The sixth section covers devices in topological quantum information processing, which are different from topological devices in traditional information processing. The seventh section is about topological light amplifiers and topological light sensors, which are fundamental components to collect and convert the signals on chip. In the eighth section, an outlook on designing future on-chip topological nanophotonic devices was discussed, focusing on the following three aspects: the idea of constructing on-chip topological devices based on other systems such as Non-Hermitian, Non-Abelian and metasurface, the application of intelligent algorithms, and the realization of multiple functional topological nanophotonic integration. In the end, a summary was given to summarize the contents. In each section from the second to the seventh, a simple introduction was given before reviewing the devices, and discussions about the opportunities and challenges were given at the end, which is expected to bring new inspiration for special devices in which researchers have great interest.

This review provided an overview about the development of on-chip topological nanophotonic devices in the recent decades and gave suggestions about future development, laying a foundation for the application of topology photonics to on-chip light information processing.

## 2. TOPOLOGICAL LIGHT SOURCES

On-chip light source provides light signal through emitting special wavelength on chip. However, the performance of the traditional on-chip light source is generally degraded when there exist disorders and defects. Topological photonics has greatly promoted the development of on-chip light sources based on topological states, such as topological lasers and topological quantum light sources, which are inherently robust against external disorders. In this section, we will review the recent progress of on-chip topological light sources.

**2.1. Topological lasers** Single mode, small divergence angle, low threshold, and high efficiency are important characteristic properties of on-chip lasers, which determine whether they possess high performance as on-chip light sources for numerous applications. The study of topological phase of

light opens up a new insight for designing disorder-immune compact on-chip light sources. Topological photonic cavities are the basic platforms for on-chip topological lasers, which benefit from non-trivial band topology and topological states. The realization of on-chip topological lasers will have wide applications in near-field spectroscopy, free-space optical sensing, electrically driven laser sources and photonic-crystal surface-emitting laser. In the current work, several kinds of typical topological lasers based on photonic Quantum Hall effect<sup>28</sup>, non-Hermitian topology<sup>29,30</sup>, valley Hall effect, photonic quantum spin Hall effect<sup>32-35</sup> and high-order topological state<sup>36</sup> are summarized, respectively.

Single mode is an important characteristic for on-chip lasers, thus many efforts have been made to realize single-mode topological lasers. In 2017, Bahari et al. realized nonreciprocal single-mode lasing based on topological cavities made of yttrium iron garnet (YIG) materials, which could operate at room temperature and telecommunication wavelengths<sup>28</sup>. Based on the YIG substrate, the time-reversal symmetry in the system could be broken under a static magnetic field. Topological cavities with arbitrary shapes were designed and experimentally realized, as shown in Fig. 2a. Their work provided the opportunity to develop complex topological circuitry of arbitrary geometries for photonic integration. However, the spectral band gap induced by magneto-optic effects is narrow, and the magneto-optic effects is very weak at optical frequencies. It is necessary to realize single mode topological lasers without adding external magnetic field.

In 2018, Bandres et al. reported the observation of topologically protected edge-mode lasing in non-Hermitian system without magnetic fields, which is based on adding gain and loss to InGaAsP quantum wells platform<sup>29</sup>. The proposed structure consisted of a 10 unit cell-by-10 unit cell coupled ring-resonator array on an active platform involving InGaAsP quantum wells. Each ring resonators were coupled to each other through link rings, and the link rings were anti-resonant to the main ring resonators. The intermediary links were judiciously spatially shifted along the y axis and introduced an asymmetric set of hopping phases, providing the lattice with a synthetic magnetic field and topological bandgaps. Laser characteristics of the topological array is shown in Fig. 2b under their full perimeter is selectively pumped, which provides a route for developing a new class of active topological photonic devices.

In addition to the property of single mode, electrical pumping performance plays a key role in practical applications. In 2020, Zeng et al. demonstrated an electrically pumped terahertz quantum cascade laser based on topologically protected valley edge states<sup>31</sup>. As shown in Fig. 2c,

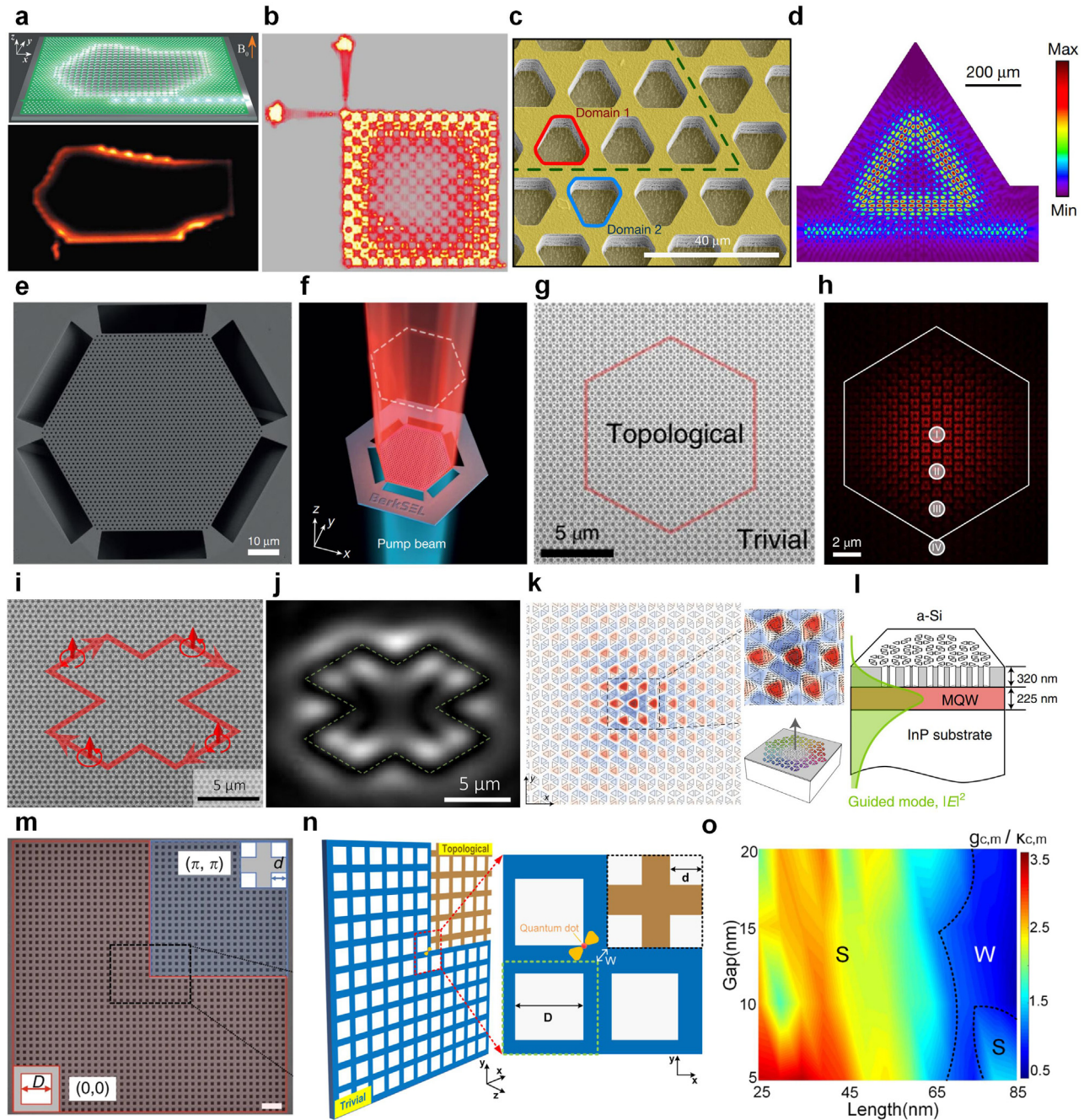


**Fig. 2** | **a**, A schematic of the topological cavity with arbitrary shapes and real-space camera image of the top of the topological cavity<sup>28</sup>. **b**, Lasing characteristics of the topological micro-resonator array<sup>29</sup>. Reprinted with permission from ref.<sup>28-29</sup>. © 2017, 2018 American Association for the Advancement of Science. **c**, SEM image of the fabricated topological waveguide near the corner<sup>31</sup>. **d**, Intensity distribution for an eigen-mode of the topological triangular loop cavity<sup>31</sup>. Reprinted with permission from ref.<sup>31</sup>. © 2020 Nature Publishing Group. **e**, SEM image of the scalable open-Dirac electromagnetic cavity<sup>37</sup>. **f**, Schematic of a Berkeley surface-emitting laser<sup>37</sup>. Reprinted with permission from ref.<sup>37</sup>. © 2022 Nature Publishing Group. **g**, The SEM image of a fabricated topological bulk laser. Reprinted with permission from ref.<sup>32</sup>. © 2020 Nature Publishing Group. **h**, Electric field distribution of a confined cavity mode. Reprinted with permission from ref.<sup>32</sup>. © 2020 Nature Publishing Group. **i**, The SEM image of a topological vortex laser with X-shaped cavity<sup>33</sup>. **j**, Lasing emission pattern of the topological vortex laser<sup>33</sup>. Reprinted with permission from ref.<sup>33</sup>. © 2020 The American Physical Society. **k**, Near fields of the Dirac-vortex topological cavity<sup>34</sup>. **l**, A schematic of the Dirac-vortex topological-cavity surface-emitting laser<sup>35</sup>. **m**, The SEM image of a fabricated topological photonic crystal corner state cavity and lasing behavior of the corner state<sup>36</sup>. Reprinted with permission from ref.<sup>34-36</sup>. © 2020 Nature Publishing Group. **n**, A schematic of the topological hybrid nanocavity<sup>38</sup>. **o**, Color map of coupling phase transition<sup>38</sup>. Reprinted with permission from ref.<sup>38</sup>. © 2021 Optica Publishing Group. (For interpretation of the references to color in this figure legend, the reader is referred to the web version of this article.)

a topological interface (green dashed line) is generated by jointing two domains of opposite valley Chern numbers together. The electric field of valley edge states is concentrated in the interface. The topological laser based on valley photonic crystal is designed by introducing a straight valley edgy-state waveguide below the bottom arm of the triangle loop cavity. The intensity distribution of a typical topological eigenmode and the spectra for the topological lasing mode are shown in Fig. 2d. The laser based on valley edge states may open routes to the practical use of topological protection in electrically driven laser sources.

Single-mode surface-emitting lasers play an important role in science and technology, such as in virtual reality systems and lasers for imaging. However, whether the single mode operation can be preserved or not depends on the cavity size. How to realize a ‘scale invariant’ cavity remains a challenge.

Recently, Contractor et al. have proposed and demonstrated a scalable single-mode surface-emitting laser (Berkeley surface-emitting lasers) based on an open-Dirac electromagnetic cavity<sup>37</sup>. The SEM image of the proposed structure is shown in Fig. 2e, where a hexagonal lattice photonic crystal is truncated to form an open-Dirac electromagnetic cavity. The free-standing cavity is connected to the main membrane by six bridges at the corners of the hexagon for mechanical stability. The single mode lasing is maintained as the size of the cavity increases because the free spectral range in open-Dirac cavities towards a constant is governed by the loss rates of distinct Bloch bands. The unconventional open-Dirac cavity mode synchronizes all unit cells (or resonators) in phase, and all unit cells take part in lasing mode. As shown in Fig. 2f, the schematic of a Berkeley surface-emitting laser illustrates the pumping beam (blue) and the lasing beam (red) from an unconventional open-Dirac cavity mode. This work demonstrates the fundamental importance of openness and mode admixtures in reciprocal space for enabling scaling in optics. The proposed open-Dirac cavities unlock avenues for light-matter interaction and cavity quantum electrodynamics.

The group of Ma et al. proposed a single-mode topological bulk laser and a topological vortex laser in micro/nano scale based on all dielectric quantum spin Hall analogy topological photonic crystal<sup>32,33</sup>. By exploring the physics of band structures from different angles, topological lasers with different merits can be realized respectively. As shown in the scanning electron microscope (SEM) image Fig. 2g, the designed single mode topological bulk laser is composed of a topological photonic crystal with quantum spin hall effect surrounded by a trivial photonic crystal. The topological interface is marked by a red line. By arranging the trivial unit nanocavity and topological unit nanocavity together on the same chip, band inversion reflection happens on the interface due to bulk band inversion at the  $\Gamma$  point. The light wave is reflected at the interface forming effective cavity feedback for lasing, because the states in the trivial photonic crystal cannot propagate into the topological photonic crystal. Fig. 2i shows the full-wave simulated fundamental cavity mode at the low-frequency side of the bandgap where the electromagnetic field is well confined in the topological bulk laser cavity. Topological vortex laser is also realized based on two kinds of spin-momentum-locked edge states, which has opposite momenta with opposite spin respectively<sup>33</sup>. The SEM image of the fabricated topological vortex laser with X-shaped topological interface is shown in Fig. 2i. As shown in Fig. 2j, the emission at the topological interface is suppressed and appears as a dark ‘X’, Their work indicates the possibility of exploiting the bulk band structures with non-trivial topology, which may be useful for collecting topological effects in bulk states beyond the edge and interface effects explored so far.

The group of Lu proposed a single mode Dirac-vortex topological cavity based on Jackiw-Rossi zero modes, which is constructed by applying a generalized Kekulé modulation in the supercell of honeycomb photonic crystal<sup>34</sup>. The near field distribution of the topological zero mode

with Dirac vortex is shown in Fig. 2k. The proposed Dirac vortex cavity could offer a robust single mode and have the largest free spectral range (FSR) among all known conventional cavities. Based on the Dirac vortex topological cavity, a best-reported performance topological-cavity surface emitting laser is realized (see Fig. 2l, exhibiting 10 W peak power, sub-1° divergence angle and 60 dB single-mode suppression<sup>35</sup>). Benefiting from the above advantages, it has great potential to achieve on-chip application.

Low threshold and high energy efficiency on-chip lasers are of great significance for the development of topological nanophotonic circuitry. In 2020, Zhang et al. demonstrated a low-threshold topological nanolaser based on the corner state<sup>36</sup>. The fabricated topological nanolaser is shown in Fig. 2m, it consists of two kinds of photonic crystal slabs with square air holes, which have the same lattice constant but different unit cells. The two kinds of unit cells have a common band structure but different 2D Zak phase,  $\theta^{Zak}$ . The electric field profile of topological corner state is shown in the inset, which is tightly localized around the corner. The experimental demonstration of a low-threshold topological nanolaser in this work will be of significance for the development of topological nanophotonic circuitry for the manipulation of photons in classical and quantum regimes. However, it is difficult for the mode volume  $V$  of the proposed structure to decrease due to light diffraction limit, making the figure of merit  $Q/V$  not high and couldn't support strong coupling.

Nanoparticle systems play an important role in studying light-matter interaction at the nanoscale. The combination of topological photonics and nanoparticle systems provides a new avenue for exploring topological phases<sup>39</sup>. In 2021, the group of Lu et al. proposed a topological hybrid nanocavity with ultra-high figure of merit  $Q/V$ , which consists of a topological photonic crystal nanocavity and a plasmonic nano-antenna (shown in Fig. 2n<sup>38</sup>). The value of the  $Q/V$  is two orders more than the bare topological photonic nanocavity and it enables the coupling between light and a single emitter to enter a strong coupling region. The coupling strength and figure of merit are controllable by adjusting the length and gap of plasmonic nano-antennas. Consequently, a coupling phase transition between weak coupling and strong coupling is achieved (shown in Fig. 2o). The variation of  $Q/V$  with the length and gap of antennas are also calculated (shown in Fig. 2o). The work provided a new method to achieve strong coupling and coupling phase transition between light and a single emitter, which will promise broad applications in quantum optics.

**2.2. Topological quantum light sources** Quantum light sources are of important applications in quantum communication, quantum information processing and quantum precision measurement. Most single photon sources rely on spontaneous parametric processes, which can be mediated by vacuum fluctuations of the electromagnetic field<sup>40–42</sup>. However, the disorders caused by nano-photonic fabrication contribute to spectral variation, seriously affecting the spectrum of generated photons. How to realize a quantum light source based on a topologically robust electromagnetic mode remains a core problem to be resolved.

The rich topological physics in coupled ring resonator systems has attracted more and more attention in recent years. Ao et al. revealed the topological phase transition in a two-dimensional coupled-resonator optical waveguide system with gain and loss<sup>43</sup>. As shown in Fig. 2a, topological phase transition occurs along the horizontal blue line with the variation of coupling strength  $\gamma$ , and vertical green line with the variation of gain-loss quantity  $\kappa$ . The electric field distributions under different gain-loss quantities  $\kappa$  are shown in Fig. 2b. When  $\kappa = 0$  and  $\kappa = 0.322$ , the system is in topological region, as shown in the two graphs above. The two graphs below in Fig. 3b show that the system evolves into a bulk state ( $\kappa = 0.761$ ) and trivial region ( $\kappa = 0.804$ ), respectively. This work provides a new degree of freedom to control topological states.

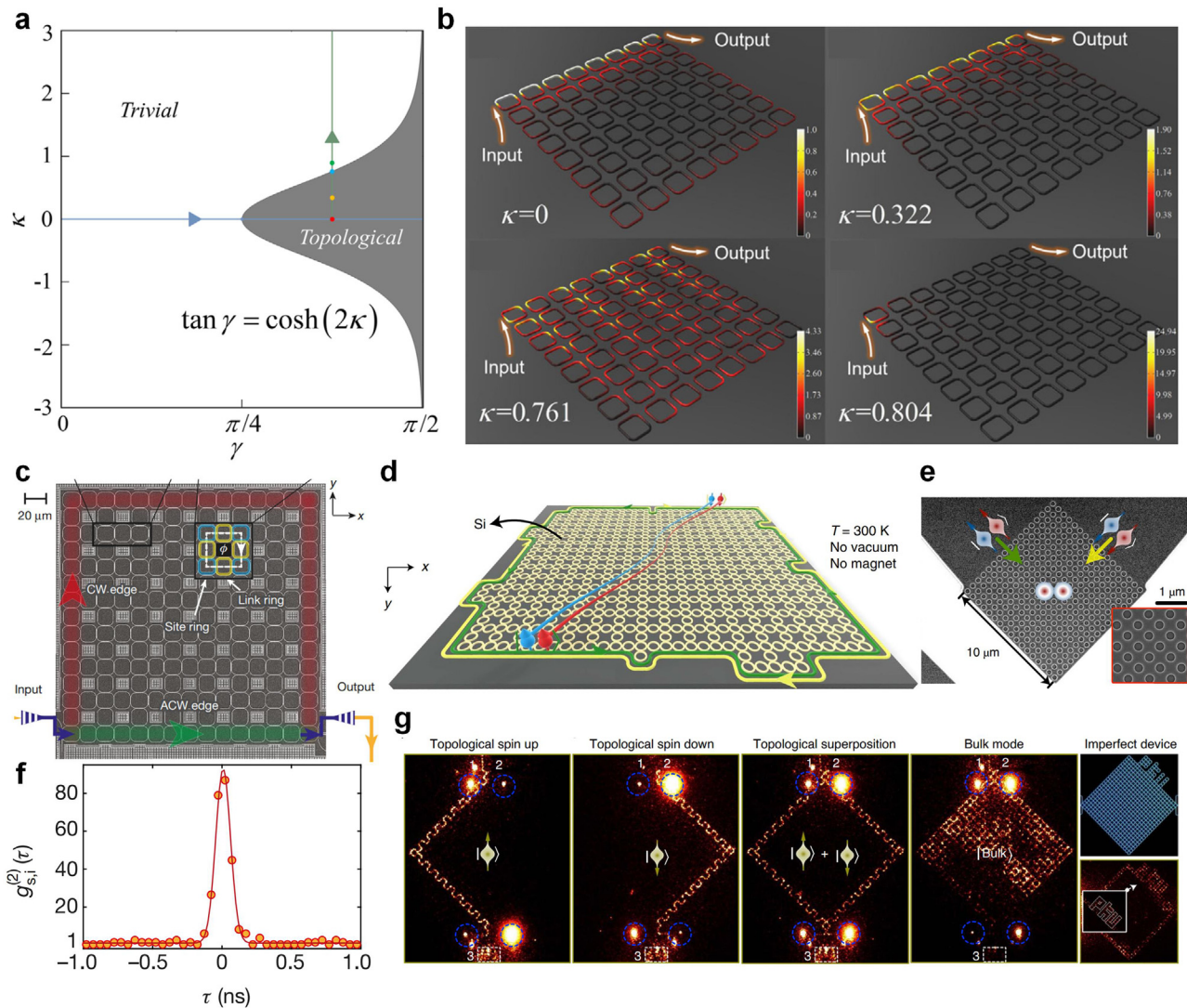


**Fig. 3** | **a**, Topological phase diagram of coupling strength  $\gamma$  and gain-loss quantity  $\kappa$ <sup>43</sup>. **b**, The electric field distribution under different gain-loss quantities  $\kappa$ <sup>43</sup>. **c**, Reprinted with permission from ref.<sup>43</sup>. © 2020 American Physical Society. The SEM image of site-ring resonators (cyan) and coupled using link rings (yellow). Reprinted with permission from ref.<sup>40</sup>. © 2018 Nature Publishing Group. **d**, Diagram of a topological quantum device in which entangled photons emerge and flow at a pair of edge modes whereas they insulate and dissipate in the bulk lattice<sup>41</sup>. **e**, 2D grating coupler consisting of periodic array of air holes<sup>41</sup>. Reprinted with permission from ref.<sup>41</sup>. © 2022 Nature Publishing Group. **f**, Histogram for the cross-correlation function  $g_{s,i}^{(2)}(\tau)$  between signal and idler photons. Reprinted with permission from ref.<sup>40</sup>. © 2018 Nature Publishing Group. **g**, Measured real-space distributions of electromagnetic fields in different modes: topological pseudospin-up edge mode<sup>41</sup>. Reprinted with permission from ref.<sup>41</sup>. © 2022 Nature Publishing Group. (For interpretation of the references to color in this figure legend, the reader is referred to the web version of this article.)

In 2018, Mittal et al. demonstrated correlated photon pairs generation by using a topological edge state realized in a two-dimensional array of ring resonators<sup>40</sup>. The SEM image of the proposed structure is shown in Fig. 3c, it consists of two-dimensional square lattice of ring resonators, which contains site-ring resonators (cyan) and coupled using link rings (yellow). A uniform magnetic field was synthesized by using link rings to couple the neighboring site rings so that a photon hopping from one lattice site to its neighbor experiences a position-dependent and direction-dependent hopping phase. The non-trivial nature of correlations between the generated photons was characterized by second-order cross-correlation function  $g_{s,i}^{(2)}(\tau)$ . A maximum  $g_{s,i}^{(2)}(\tau) \approx 80$  at  $\tau = 0$  is observed (Fig. 3f), which is different from the condition of two uncorrelated sources ( $g^{(2)} = 1$  for all  $\tau$ ). The topological source of quantum light

is promising to pave the way for the development of robust quantum photonic devices, which is of broad applications in quantum communications.

Recently, Dai et al. demonstrated on-chip topological protected quantum entanglement emitters, which could generate topological protected entanglement and immunity against the environmental perturbations<sup>41</sup>. The diagram of the proposed structure is shown in Fig. 3d, it consists of a  $10 \times 10$  lattice of strongly coupled micro-ring resonators and supports two counter propagating edge states (CCW and CW) in the site rings. A 2D grating coupler is located at the terminal to ensure the coherent superposition of pseudospin states (Fig. 3e). Real-space distributions of electromagnetic fields in different modes were measured, as shown in Fig. 3g, and the robustness of the device was also demonstrated by introducing defects arranged in a ‘PKU’ shape. The topologically protected quantum entan-

lement emitters can promote the research of other topological quantum photonic sources and are promising to be applied in quantum computation.

**2.3. Opportunities and challenges** The development of topological photonics has greatly promoted the generation of high performance on-chip topological light sources. They are robust to perturbations and possess the performances of pure single-mode, small divergence angle, low threshold and high energy efficiency. All of the advantages above ensure that the topological light source have wide application in near-field spectroscopy, free-space optical sensing, photonic-crystal surface-emitting laser, quantum communication and quantum computation. However, for the realization of photonic chip, two existing challenges still remain to be resolved: the first is how to integrate the topological light source with other on-chip functional optical device; the second is how to increase the energy conversion efficiency or reduce the energy loss between these devices. For the first concern, it is determined by the progress in micro/nano fabrication technology in the future. For the second concern, maybe the method of inverse design could optimize the efficiency problems.

### 3. TOPOLOGICAL LIGHT WAVEGUIDING

Topological photonics emerges as a novel route to manipulate the flow of light. Topologically protected photonic states, which are supported at the interface of trivial and topologically nontrivial insulating structures, play an important role in enabling low-loss optical waveguides in the presence of structural imperfections. Since the first discovery of robust optical waveguides in the microwave regime by using photonic chiral edge states<sup>9</sup>, topologically protected wave propagation based on topological edge states in photonic quantum Hall effect, photonic quantum spin Hall effect, photonic Valley Hall effect and photonic Floquet Hall phase, have been observed not only in microwave<sup>44–48</sup>, but also in the optical and near-infrared range<sup>49–52</sup>. Below, we will discuss some typical achievements of topological photonic waveguides.

**3.1. Topological waveguides based on photonic quantum Hall effect** Haldane and Raghu theoretically demonstrated that a photonic crystal with broken time reversal symmetry could exhibit photonic analogue of the quantum Hall effect<sup>7,53</sup>. The chiral edge states could travel only in one direction along the boundary of two photonic crystals forming a waveguide, even in the presence of structural imperfections and sharp bends. The first theoretical<sup>8</sup> and experimental<sup>9</sup> photonic quantum Hall effect was verified by Wang et al. in gyromagnetic photonic crystals. Fig. 4a (top) shows the calculated light propagation field diagram<sup>9</sup>. It can be clearly seen that the forward propagation of light is almost not subject to the backscattering of obstacles. The forward and backward transmission spectra measured in the experiment are shown in Fig. 4a (bottom), and the huge differences between them prove the robust propagation of chiral edge states.

Subsequently, several experimental works were also reported based on the gyromagnetic photonic crystal platform<sup>19,45,54,55</sup>. A hybrid approach was adopted to break the time-reversal symmetry of a semiconductor photonic crystal under a static external magnetic field<sup>28</sup>. They bonded a photonic crystal slab with InGaAsP quantum multiple wells on an YIG film. In addition, topological nontrivial gaps and edge states are proved in amorphous systems (Fig. 4b)<sup>56</sup>.

**3.2. Topological waveguides based on photonic quantum spin Hall effect** Magneto-optical effect is limited to microwave frequencies and tends to be very weak in the optical range<sup>57</sup>. Difficulties in applying magnetic fields and the scarcity of gyromagnetic materials make it difficult to realize the

photonic quantum Hall effect. The challenges of breaking time reversal symmetry have stimulated the search for the photonic analog of quantum spin Hall (QSH) effect in time-invariant systems<sup>58</sup>. The edge states at the QSH topological systems have some different features from the quantum Hall systems. Firstly, the edge states are no longer one-way transmission, and light can travel either forward or backward. Furthermore, quantum spin Hall systems are characterized by Z<sub>2</sub> topological invariants. The robustness of edge states against sharp bending, random distribution of synthetic gauge field, and lattice disorder have been experimentally verified.

Photonic QSH states were theoretically proposed by Hafezi et al. in 2011 using a network of coupled resonator optical waveguides (CROW) in two dimensions, which produced phase shifts that were non-commensurate with the lattice<sup>59</sup>. This proposal was realized experimentally in 2013<sup>50</sup>, and other schemes were proposed using optical ring-resonators soon<sup>60</sup>. Additionally, QSH effect could also be realized in bi-anisotropic metamaterials (Fig. 4c). In this case, the spin components were represented by two linear combinations of transverse electric (TE) and transverse magnetic (TM) modes. Compared with CROW, the bi-anisotropic metamaterials could be fabricated at the same order of size as the electromagnetic wavelength<sup>61</sup>.

Recently, a different method based on all-dielectric materials to implement an analog of the quantum spin Hall effect for photons in two dimension has been proposed theoretically<sup>65</sup> and realized experimentally<sup>62</sup> by Hu and Hang group, which was friendly to on-chip integration in the optical range. The configuration was based on all-dielectric materials, and QSH effect could be induced by deforming honeycomb lattices of rods into triangular lattices, as depicted in Fig. 4d. The simplicity of this proposal has triggered the implementation in other photonic systems, such as microwaves (Fig. 4e)<sup>46</sup>, and photonic crystal slab (Fig. 4f)<sup>63</sup>.

**3.3. Topological waveguides based on valley Hall effect** Another structure that can construct topological waveguide is valley photonic crystal, which is photonic analogue of the valley Hall electronic system. The photonic valley Hall effect was firstly proposed by breaking the spatial inversion symmetry of triangularly arranged dielectric rods, and the unidirectional propagation of edge states and efficient in-coupling and out-coupling were also demonstrated<sup>66</sup>. The valley-dependent robust propagation was experimentally observed in microwaves using designer surface plasmon crystals (Fig. 4g)<sup>47</sup>, and was further extended to surface waves based on photonic crystals (Fig. 4h)<sup>64</sup>.

Silicon-on-insulator (SOI) platform, which is compatible with complementary metal oxide semiconductor (CMOS) technology and allows integration with other optoelectronic devices on a single chip, is a widely used platform in silicon photonics. The robust light propagation in an SOI valley photonic crystal waveguide was experimentally realized in 2019<sup>67</sup>. Slow-light effect has attracted wide interests of researchers due to the fact that it could increase light-matter interaction and enhance linear and nonlinear effects<sup>68–72</sup>. The theoretical study suggested that the valley-protected slow lights were more robust than trivial waveguides against the disorder<sup>70</sup>. It is of great significance to combine slow light waveguides with topological nontrivial edge states, enabling a lot of possible applications in optical signal processing devices<sup>71,72</sup>.

**3.4. Topological photonic waveguide arrays** Topologically protected photonic states have been experimentally studied by making use of one-dimensional SSH-model-based coupled silicon waveguide arrays<sup>20</sup>. The structure was fabricated by connecting two silicon waveguide dimer chains with different topological invariants, and the topological transition would occur at the interface between them. The single topological state formed by the long-long defect can be translated to the compound trivial state which exists at the short-short defect by varying the configuration of

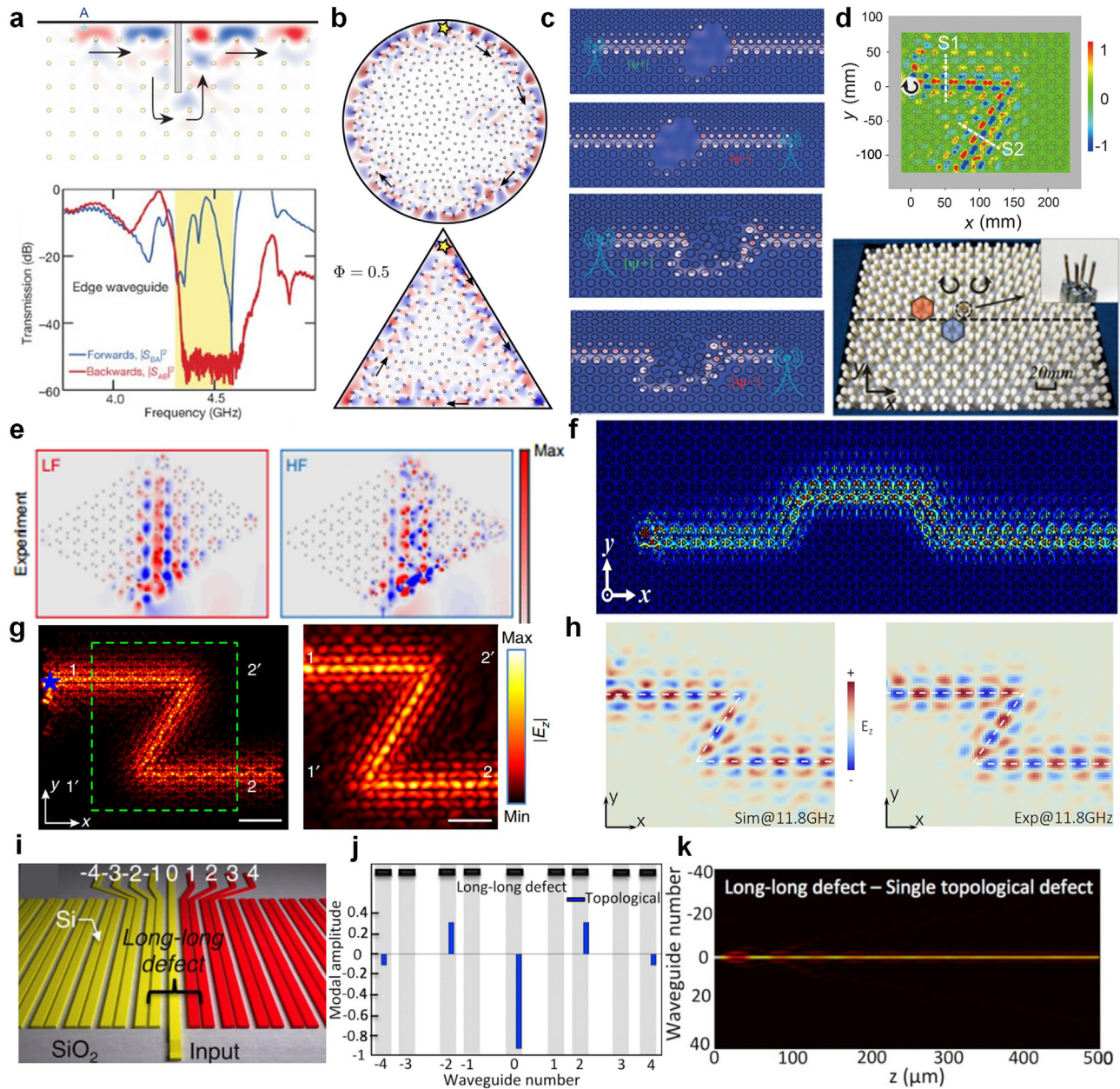


**Fig. 4 | Topological photonic waveguides in 2D platform.** **a**, The topological waveguide which show the robust transmission of light with little backscattering (top), and the measured transmission spectra of forward and backward light (bottom). Reprinted with permission from ref.<sup>9</sup>. © 2009 Nature Publishing Group. **b**, Robust TM edge propagation in amorphous lattices<sup>56</sup>. **c**, Excitation of surface waves by a point dipole source at the interface between topologically trivial and non-trivial photonic insulators<sup>61</sup>. Reprinted with permission from ref.<sup>56,61</sup>. © 2017, 2013 Nature Publishing Group. **d**, The robust transport of the out-of-plane electric field. Reprinted with permission from ref.<sup>62</sup>. © 2018 American Physical Society **e**, Experimental electric field maps for the LF and HF edge modes. Reprinted with permission from ref.<sup>46</sup>. © 2017 Nature Publishing Group. **f**, Electric field intensity for an edge state with four bends. Reprinted with permission from ref.<sup>63</sup>. © 2016 Institute of Physics Pub. **g**, Valley-dependent robust propagation experimentally observed in microwaves using designer surface plasmon crystals. Reprinted with permission from ref.<sup>47</sup>. © 2017 Nature Publishing Group. **h**, Topological protection of the edge state in a Z-shaped waveguide<sup>64</sup>. **i**, Two silicon dimer chains connected by a long-long defect<sup>20</sup>. **j**, Modal amplitude of the topological defect mode for the long-long defect case<sup>20</sup>. **k**, Propagation simulations of the input signal propagating through the structures of Fig. 4i<sup>20</sup>. Reprinted with permission from ref.<sup>20,64</sup>. © 2016, 2017 American Physical Society.

the waveguides between the interfaces. The structure with the long-long defect and the modal amplitude of single topological modes around the defect are shown in Fig. 4i and Fig. 4j. Fig. 4k depicts the propagation of lights in the singular topological defect, and the lights are always being exponentially localized around the defect. This work provided experimental

evidence for topologically protected waveguides based on coupled silicon waveguide arrays.

The Floquet topological phase can be understood as a time counterpart of the Bloch theorem, which means that a solution of a time-periodic Hamiltonian can be expressed by multiplying a time-periodic function by

a phase term. Just as spatially periodic structures can possess a topological phase, a system under periodic temporal modulation can also support a topological phase called the Floquet topological phase<sup>73,74</sup>. This phenomenon has also been realized in photonics by using time-dependent index modulation<sup>75,76</sup> and using the propagation axis of a waveguide array to mimic a time-like axis<sup>77,78</sup>.

Coupled helical waveguides arranged in a graphene-like honeycomb lattice have recently been investigated experimentally<sup>49</sup>, and the experimental results clearly confirmed that the twisting of the waveguides produced a topological Floquet state, resulting in a topological edge state at the open ends of the waveguide array. The robustness of the edge state was also confirmed by reflectionless propagation across sharp corners between different cuts of the lattice and around the waveguide with defects. The discovery of a rigorous mathematical connection between Floquet topological systems and two-dimensional networks of ring resonator arrays provided a mechanism for direct mapping and emulation of Floquet states in this platform<sup>79</sup>. Recently, another so-called anomalous Floquet insulators,<sup>79,80</sup> have been demonstrated experimentally by lifting the condition of fast modulation<sup>77,78</sup>.

**3.5. Opportunities and challenges** Topological edge states were also demonstrated in higher-dimensional and non-Hermitian photonic systems. Photonic platforms that can support topological systems exist in a wide range of frequencies, providing more possibilities for the design of on-chip photonic devices in Hermitian and non-Hermitian systems in the future. Of course, there is an upper limit to the robustness of topological structures, which means the transmission of light will be affected by strong disturbance. Due to the limitation of the size of platform and other technical issues, it still remains difficult to realize the transformation of miniaturization to the nanoscale. Therefore, great challenges will be continuously faced in the research of topological photonic waveguide in the future.

## 4. TOPOLOGICAL LIGHT DIVISION AND SELECTION

In information processing on optical chips, light division and selection devices are very important because they can be used for broadband information processing, dividing lights with different information and allocating them to different position or ports. Traditional devices based on topologically trivial nano-structures are sensitive to errors, disorders, and even imperfect fabrication, whose performances will be seriously affected by structure deviations. The introduction of topological photonics presents a good platform to design robust topological light division and selection devices. Here, topological light division devices include topological rainbow, topological routers, and topological power splitters. Topological light selection devices mainly refer to topological filters.

**4.1. Topological rainbow** Topological rainbow, which can separate, slow and trap topological photonic states of different frequencies into different positions, was firstly proposed and achieved in synthetic dimensional topological photonic crystal systems by Lu et al.<sup>81</sup>. Before topological rainbow, researchers have paid more attention to the special edge mode and rich physical phenomenon of topological states instead of multiple wavelengths of topological photonic states, which cannot satisfy the increasing needs of on-chip broadband information processing of topological states in the Big Data era. As shown in the first row of Fig. 5a, the synthetic dimension was introduced into the system by employing the translational degree of freedom of nanostructures in the unit cell. The deformation of the translational degree of freedom will result in topological

states in the synthetic parameter space<sup>81</sup>. The group velocities of the topological states can be controlled by modulating of dispersion, and the slow light effect of topological states can be realized by reducing the speed of light propagation to zero through synthetic dimension, which can be seen from the second row of Fig. 5a. The topological rainbow based on synthetic dimension has no restrictions for symmetries, lattice types, materials, wavelength band, and is easy for on-chip integration. Especially, it provides a reliable method for the on-chip topological photonic states with multiple wavelengths based on all-dielectric materials in the optical frequencies range.

The first experimental realization of on-chip topological rainbow at the nanoscale was given by Lu et al., which is shown in Fig. 5b<sup>82</sup>. The device consisted of two regions, the dispersing region (denoted with blue color) and barrier regions (denoted with red color). The dispersing region was used to divide topological states with different wavelengths to different positions. The barrier region was used to limit light in the device. Light with wavelengths within the bandgap of trivial photonic crystals was injected from the right side through a waveguide and was dispersed by the designed structure to different positions. The SEM image was shown in the first column of Fig. 5b. The measured results by scanning near-field optical microscope were shown in the second column of Fig. 5b. It can be seen that topological states with different wavelengths were localized at different positions. The work provided an effective method to detect on-chip topological photonic devices with multiple frequencies at the nanoscale.

Another method to achieve topological rainbow is building graded structures along the topological interface. Zhang et al. designed a topological rainbow by gradually contracting and expanding the lattice<sup>83</sup>. By shrinking and expanding the dielectric cylinders from the center of hexagon, doubly degenerate Dirac cones will be opened. Topological rainbow can be achieved by putting the expanded and contracted lattice on the opposite sides of the interface. The graded structures and the simulated results of topological rainbow trapping effects are shown in Fig. 5c. Light with frequencies within the bandgap was injected from the left port and separated into different positions according to frequencies. Elshahat et al. proposed a structure to realize multiple topological rainbows by inserting sandwiched gradient structure as a coupling region in the topological photonic crystal waveguide, as shown in Fig. 5d<sup>84</sup>. In addition, the coupling area can generate unique topological edge states by introducing multi-line topological waveguides. A one-way topologically protected slow-light coupling state with low group velocity, bandwidth-broadening and robust transmission was introduced. Due to the coupling between different modes in the multi-line topological waveguides, energy exchange existed in the coupling area during the transporting process. Besides, they showed that the system could be reconfigured to rainbows of different shapes as shown in Fig. 5d, which are essential in practical application.

Besides, Li et al. proposed a topological rainbow based on a sandwiched dual-mode topological waveguide, which was made by putting non-trivial photonic crystals between two regions of trivial photonic crystals<sup>85</sup>. Mao et al. designed a topological rainbow using valley photonic crystals<sup>86</sup>. They tuned the distance between cylinders in two regions on the opposite sides of the interface gradually to form a topological rainbow. Recently, Liang et al. have showed that the topological rainbow can also be designed with higher-order topological corner modes (HOTCMs)<sup>87</sup>. They found that the HOTCMs with different geometry configurations have different dispersive properties, which is the start point of designing topological rainbow with HOTCMs. Elshahat et al. also reported a bidirectional rainbow trapping, which are realized based on trapping a chirped photonic crystal as a sandwich between two edge states<sup>88</sup>. This work provided a new way to construct topological nanophotonic devices.

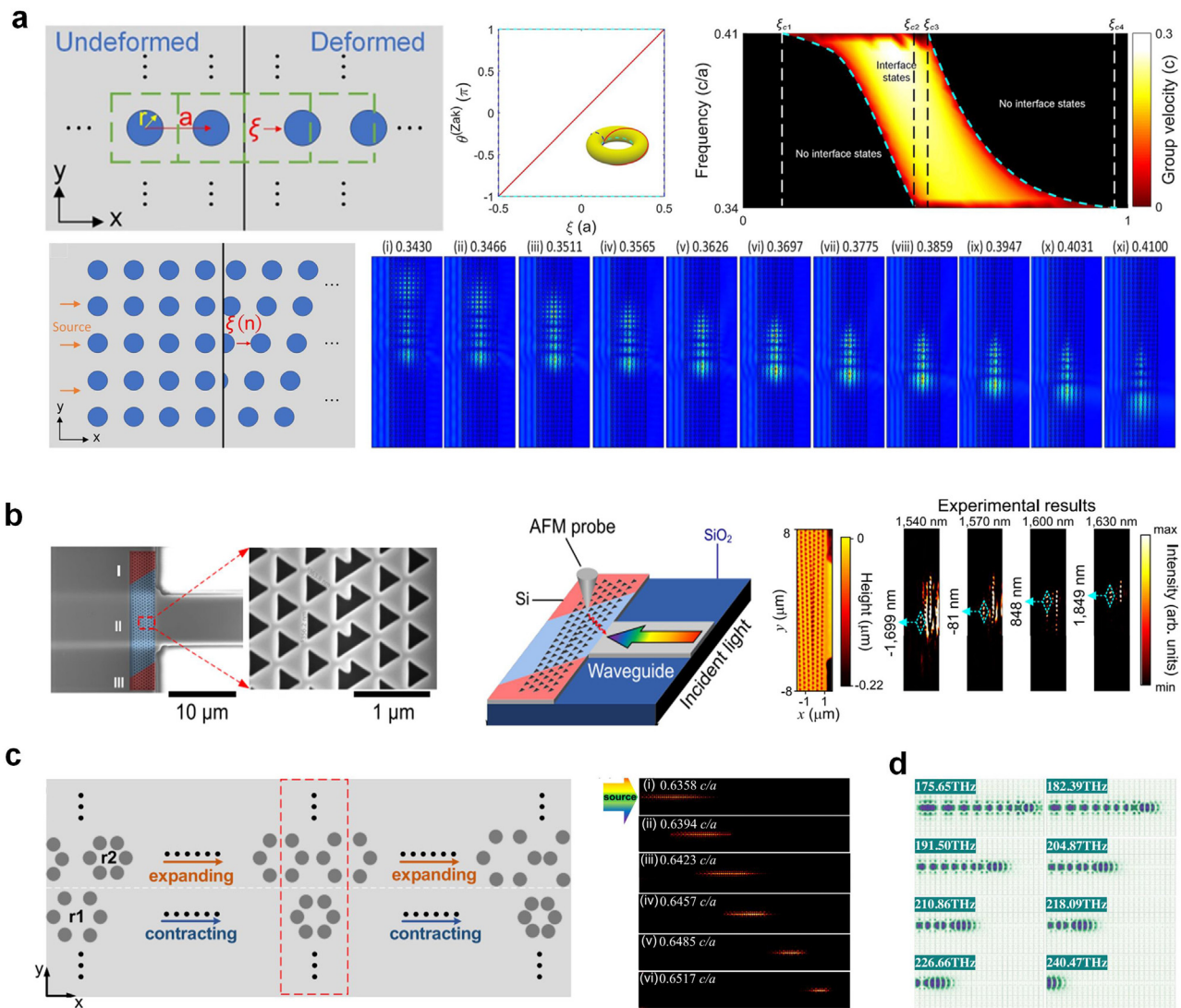


**Fig. 5 | Topological rainbow.** **a**, Topological rainbow concentrator based on synthesis dimension of translation. The group velocity distribution shown in the dispersion diagram of synthetic space. The intensity distributions in the synthetic dimensional topological photonic crystal excited by incident plane wave from the left side. Reprinted with permission from ref.<sup>81</sup>. © 2021 American Physical Society. **b**, On-chip topological rainbow samples and experimental results based on synthetic dimension. Reprinted with permission from ref.<sup>82</sup>. © 2022 Nature Publishing Group. **c**, The graded topological photonic crystal and electric field distributions of electric field for different frequencies of topological rainbow trapping device. Reprinted with permission from ref.<sup>83</sup>. © 2021 Optical Society of America. **d**, The broadband unidirectional topological rainbow. Reprinted with permission from ref.<sup>84</sup>. © 2022 Wiley-VCH.

Light information trapping and releasing are two important applications of topological rainbow. Topological rainbows, which can switch between trapping and releasing, are very important in light information dynamic access. Mao et al. designed a topological rainbow based on electro-optical material whose refractive index can be tuned by external voltage<sup>89</sup>. The topological protection was provided by valley photonic crystals.

**4.2. Topological routers** Topological routers can guide and route light, usually carrying different information, into different output ports. Traditional routers such as wavelength routers based on micro rings are sensitive to fabrication errors<sup>90</sup>. There are different topological mechanisms to achieve topological routers, including gyromagnetic materials<sup>91,92</sup>, bianisotropic photonic crystals<sup>93,94</sup>, and valley photonic crystals<sup>67,95–100</sup>.

Topological photonic crystal based on gyro-magnetic materials was firstly proposed by Wang et al.<sup>8</sup>. By adding an out-of-plane magnetic

field, time reversal symmetry was explicitly broken. In analogy to quantum Hall effect, there are topologically protected edge states occurring in the bandgap. The propagation direction was determined by the magnetic field direction. By tuning the magnetic field distribution in different regions, He et al. achieved a tunable one-way edge states router using YIG rods and Alumina rods in 2010<sup>92</sup>. As shown in Fig. 6a, YIG and Alumina were distributed to form a cross waveguide. By tuning the perpendicular magnetic field direction added to the YIG regions, the cross waveguide supported different edge modes, guiding different edge modes to different output ports.

Skirlo et al. explored the large Chern number phenomenon in topological gyromagnetic photonic crystals<sup>91</sup>. With the designed photonic crystals with large Chern number, they designed a continuously tunable power splitter, as shown in Fig. 6b. The power splitter was made of a metal wall and two kinds of topological photonic crystals with Chern numbers of +1

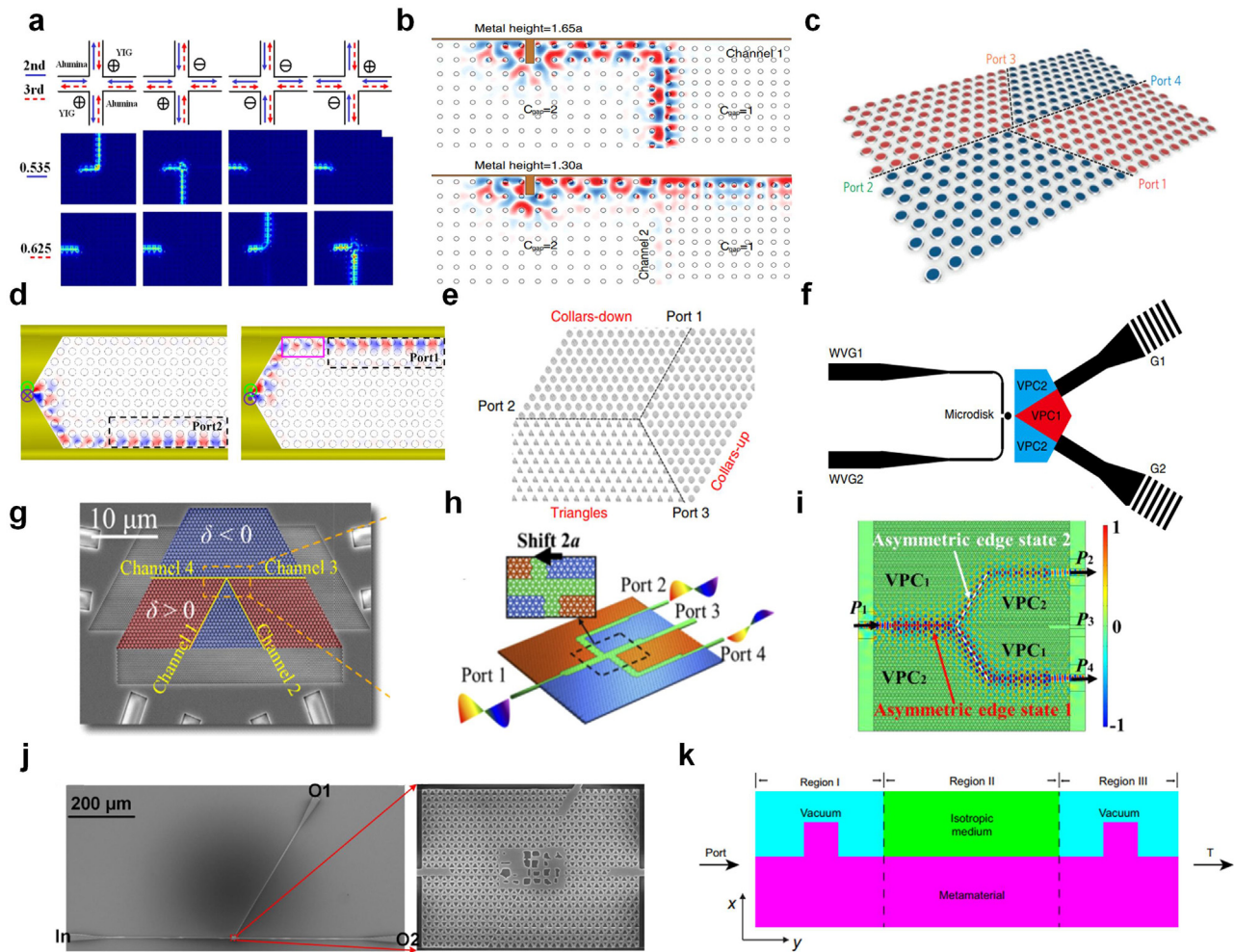


**Fig. 6 | Topological routers and power splitters. a**, Tunable edge states router based on gyromagnetic materials. Reprinted with permission from ref.<sup>92</sup>. © 2010 American Institute of Physics. **b**, Continuously tunable topological power splitter based on gyromagnetic photonic crystals with large Chern numbers. Reprinted with permission from ref.<sup>91</sup>. © 2014 American Physical Society. **c**, Topological spin-locked wave splitter based on bianisotropic materials. Reprinted with permission from ref.<sup>93</sup>. © 2016 Nature Publishing Group. **d**, Pseudospin-polarized power splitter based on topological bianisotropic metamaterials. Reprinted with permission from ref.<sup>94</sup>. © 2015 American Physical Society. **e-g**, Topological edge states routers based on valley photonic crystals<sup>67,95,100</sup>. Reprinted with permission from ref.<sup>67,95,100</sup>. © 2018, 2019 Nature Publishing Group. © 2019 Wiley-VCH. **h-i**, Topological power splitters with arbitrary ratio based on valley photonic crystals<sup>97,99</sup>. Reprinted with permission from ref.<sup>97,99</sup>. © 2022 Wiley-VCH. © 2020 Optical Society of America. **j**, Topological wavelength router based on valley photonic crystals. Reprinted with permission from ref.<sup>96</sup>. © 2021 Multidisciplinary Digital Publishing Institute. **k**, Wavelength filter based on gyromagnetic photonic crystals. Reprinted with permission from ref.<sup>101</sup>. © 2021 American Physical Society.

and +2. The light source excited light mode which was a linear combination of two edge modes. When light propagated through the metal obstacle, two edge modes would interfere with each other. The height of metal obstacle affected the interference way of these two modes and modulates these two modes to be supported by channel 1 and channel 2, which were single mode waveguides.

Besides gyromagnetic photonic crystals, optical bianisotropic metamaterials are also a candidate to achieve topological photonic system<sup>61</sup>. The key advantage of bianisotropic metamaterials is the flexibility of engineering their electromagnetic response parameters. The mechanism of bianisotropic metamaterial is analogous to quantum spin Hall effect, which supports edge states in the band gap without external magnetic field. Based on bianisotropic metamaterials, Cheng et al. realized a spin-locked wave splitter, as shown in Fig. 6c<sup>93</sup>. Two kinds of topological photonic crystals with different spin-Chern numbers formed a cross waveguide.

Pseudospin down edge mode input from port 1 and was divided into port 2 and 4. There was nearly no light transmitted to port 3. Chen et al. presented a pseudo-spin-polarized power splitter based on topological bianisotropic metamaterials<sup>94</sup>, as shown in Fig. 6d. In their device, light with different TE-TM polarization would be guided to different ports along the corresponding topological channels.

As a typical topological photonic crystal, valley photonic crystal, which provides “valley” information degree of freedom, can be constructed after opening the Dirac point by breaking spatial symmetry<sup>26</sup>. The fabrication-friendly and absence of external magnetic field make it a good platform to demonstrate topology protected photonic devices with all-dielectric materials. Based on valley photonic crystals, there are various routers and splitters reported, as shown in Fig. 6e-j.

A valley-selective topological router was presented by Kang et al. in 2018<sup>100</sup>. The structure is shown in Fig. 6e. The junction was formed with

three kinds of valley photonic crystals. In the waveguide of port 1, spin-down states at K and K' valley were supported, while port 2 and port 3 only supported spin-down state at K valley and K' valley, respectively. When spin-down states at K and K' arrived at the junction, they would be guided into different ports. He et al. explored the phase vortex features of edge states at different valleys and took advantage of their discovery to design a topological valley-charity locking router, as shown in Fig. 6f<sup>97</sup>. A sub-wavelength microdisk was used to serve as phase vortex generator. Light injected from waveguide 1 (WVG1)/waveguide 2 (WVG2) would excite anticlockwise/clockwise phase vortex in the microdisk and couple to different topological channels. The right column of Fig. 6f shows the SEM image around the microdisk for samples. Besides, Ma et al. also achieved a router of valley kink states experimentally, as shown in Fig. 6g<sup>95</sup>. Their results showed that the topological kink states had good robustness to sharp bends in routers.

There are also power splitters made with valley photonic crystals. He et al. studied the band structure of so-called ABC-type superlattice and employed it to design a power splitter with arbitrary ratio, as shown in Fig. 6h<sup>99</sup>. The ABC-type superlattice was composed of trivial photonic crystals in the middle and two kinds of valley photonic crystals separated in two sides. These two kinds of valley photonic crystals had similar symmetry but had gap at different points (K and K' in the first Brillouin zone). In Fig. 6h, the trivial photonic crystal is represented with green color while the other two kinds of photonic crystals represented with blue and orange. By tuning the shift of these three types of photonic crystals around the junction, light power allocated to different ports would be changed continuously. Wang et al. studied the asymmetric valley photonic edge states, which have asymmetric field distributions<sup>97</sup>. They demonstrated that, by tuning the geometry parameters of asymmetric valley photonic crystals, an arbitrary ratio power splitter could be achieved. Fig. 6i, as an example, shows a 1:2 power splitter.

Yuan et al. combined intelligent algorithm with valley photonic crystals to design an on-chip topological nanophotonic wavelength router working in the photonic crystal band gap around optical communication range<sup>96</sup>. The left panel of Fig. 6j shows the test platform with three waveguides connecting the designed router and the right panel is the designed device. The three topological channels, In, O1 and O2, were made with valley photonic crystals. The input light entered the structure from the left edge and was divided by the central region. Light with different wavelengths of topological photonic states would be output from O1 and O2, respectively. The central region was optimized with topology optimization. The introduction of intelligent algorithm into on-chip topological nanophotonic devices provides an effective method to predict new structures and design devices with excellent performances.

**4.3. Topological filters** Topological light filters are important light processing devices which can filter out unwanted light and leave target light protected. Gu et al. designed a wavelength-selective notch and channel-drop filter based on a topological photonic ring resonator<sup>102</sup>. The triangular ring resonator was designed using silicon-based valley photonic crystals. Two topological waveguides connect the ring at a corner of the triangle to form a junction. Input light meeting the resonating condition propagated in the topological ring to form a stable mode, leading to periodic dips on the transmission spectrum.

Han et al. studied edge states with gaps in gyromagnetic photonic crystals<sup>101</sup>. By breaking the electromagnetic duality symmetry in the system, there occurred a band gap for edge states. They designed a wavelength filter with this kind of photonic crystal, as shown in Fig. 6k. The spectrum in the left panel shows that this kind of topological photonic crystals have good filtering effects for light with frequencies in the gap. The structure diagram of their designed filter is shown on the right panel

of Fig. 6k. Furthermore, the filter bandwidth can be adjusted by changing the electromagnetic response parameters of the material.

**4.4. Opportunities and challenges** Owing to the steering ability of light with different wavelengths, topological rainbow has good application potential in on-chip light processing. It is also shown that topological rainbow can switch between trapping and releasing by tuning external electric field. However, there still remain challenges for further application. The first one is large bandwidth. Due to the fact that the working wavelength range usually lies in the bandgap, the bandwidth is no larger than the bandgap. Secondly, dynamic with the external magnetic field is not beneficial for on-chip integration. Much more efforts should be made in the development of concepts and theory to achieve broader application of topological rainbow.

Routers based on different topological protection mechanisms are of different features. Devices based on magnetic-optic effect are easy to be tuned with external magnetic field, which is suitable for active tunable devices. In addition, routers based on valley photonic crystals are easy to achieve and to be integrated. The silicon-based valley topological routers are compatible with currently integrated circuits technology, which is beneficial for minimization and integration. Moreover, polarization splitting of routers based on bianisotropic metamaterials could be achieved theoretically by designing the electromagnetic response of materials. However, there are still challenges for the development of topological routers. Firstly, the external magnetic field brings inconvenience for on-chip integration. Secondly, the topological protection provided by valley photonic crystals is not strong enough when compared with some other topological protection mechanisms. Thirdly, it should be pointed out that bianisotropic metamaterials are usually of complicated structures<sup>103</sup> and are not easy to be fabricated or integrated on a chip.

The reported works proved that topological photonics could be used to design topological filters which are immune to fabrication errors. Topological filters based on edge states with gaps in gyromagnetic photonic crystals have steep filtering spectra and adjustable bandwidth. However, topological filters based on topological ring resonators are of a relatively bulky size. Besides, topological filters based on edge states with gaps in gyromagnetic photonic crystals are also not easy to be implemented in the experiment.

## 5. TOPOLOGICAL LIGHT INFORMATION PROCESSING

In order to manipulate the light signals efficiently and achieve more functionalities on the photonic chip, it is necessary to build topological light circuits. Topological optical switches, topological optical isolators and circulators, topological optical logical gates, and even topological quantum light processing, which can manipulate light and deal with light information, are core components of photonic chip. In this section, typical examples of these devices mentioned above will be introduced.

**5.1. Topological optical switches** Optical switch is an essential component of photonic circuits, which is defined as a structure with external signal controlling the ON/OFF transition of light propagation. Ultrafast response time and low energy consumption are key characteristics for optical switch. Traditional all-optical switches are based on photonic crystals, surface plasmon polariton, micro-ring resonators, and metamaterials, which, however, have difficulties meeting the requirements of robustness, high speed and high-capacity information processing<sup>104,105</sup>. Studies on topological photonics help progress this traditional technology and bring robustness in switch structure.

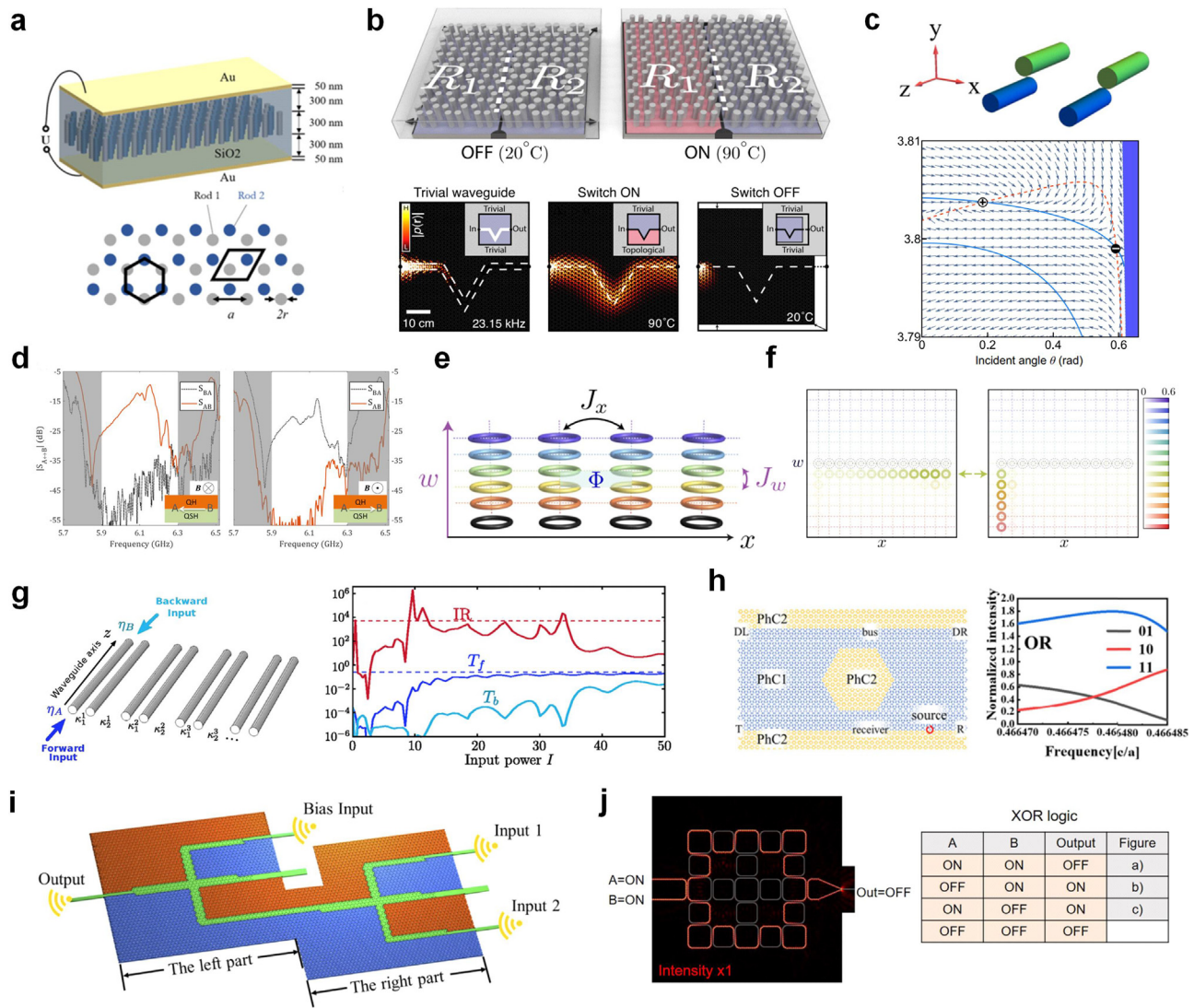


**Fig. 7** | **a**, Schematic the reconfigurable valley photonic crystal and a two-dimensional model of the valley photonic crystal composed of TiO<sub>2</sub> (rod 1, gray rods) and BaTiO<sub>3</sub> (rod 2, blue rods)<sup>106</sup>. **b**, Topological phononic switch regulated by sonic heating<sup>107</sup>. **c**, Schematic of Lorentz nonreciprocal grating with dimer unit cells<sup>110</sup>. **d**, Topological isolator based on combination of quantum Hall effect and quantum spin Hall effect<sup>111</sup>. **e**, Effective lattice made of a 1D array of resonators with coupling in a synthetic dimension<sup>114</sup>. **f**, Optical isolator based on synthetic two-dimensional lattice<sup>114</sup>. Reprinted with permission from ref.<sup>106,107,110,111,114</sup>. © 2016, 2018, 2019, 2020, 2022 American Physical Society. **g**, Optical isolation based on 1D SSH model, realized by an array of coupled waveguides. Isolation ratio (IR), forward transmittance  $T_f$ , and backward transmittance  $T_b$ , versus input power  $I$ . Reprinted with permission from ref.<sup>115</sup>. © 2017 Institute of Physics Pub. **h**, Topological optical logic gates based on two-dimensional photonic crystals<sup>116</sup>. **i**, Schematic diagram of XNOR, NAND, and NOR gates, composed of two logic inputs, a bias input, and an output<sup>99</sup>. Reprinted with permission from ref.<sup>99,116</sup>. © 2019, 2020 Optical Society of America. **j**, Demonstration of the XOR logic in the proposed device and XOR logic truth table. Reprinted with permission from ref.<sup>117</sup>. © 2021 IOP Publishing Ltd. (For interpretation of the references to color in this figure legend, the reader is referred to the web version of this article.)

Such devices can be realized in photonic crystal by applying electro-optical effect. Wu et al.<sup>106</sup> theoretically proposed an optical switch based on reconfigurable valley photonic crystal. As shown in Fig. 7a, TiO<sub>2</sub> (Rod 1, gray) and BaTiO<sub>3</sub> (Rod 2, blue) are arranged in triangular arrays to form valley photonic crystal. A Dirac point locates in the energy band diagram, due to the inversion symmetry given by the same refractive index of 2.38 between Rod 1 and Rod 2. An external voltage of 75V (−75V) gives  $n_{BTO} = 2.26$  ( $n_{BTO} = 2.5$ ) and opens a topological band gap between the first and second energy band above (below) the original Dirac point. Thus, different external voltage allows for light with different frequency to propagate through the valley photonic crystal insulator.

Another similar switch was designed using active control over phononic crystal.<sup>107</sup> Steel rods were arrayed in honeycomb lattice to form a topological trivial phase. As shown in Fig. 7b, the radii of steel rods from both sides were correctly chosen to allow active control by using ultrasonic heating. The left side phase transition varies from trivial to topological nontrivial phase when the temperature was increased from 20 °C to 90 °C, while the other side remained trivial throughout the whole process. Thus, the sonic wave did not propagate through the disorder unless the system was heated.

Topological optical switch provides a strategy to achieve faster computing and lower consumption. But active control over photonic topolog-

ical transition needs more exploration before better improvement can be applied in topological optical switches.

**5.2. Topological optical isolators and circulators** Nonreciprocal elements play an important role in photonic circuits, and two hallmark examples are optical isolators and circulators<sup>108</sup>. Optical isolators allow light to transmit in one direction but block the transmission in the other direction nonreciprocally. To build a nonreciprocal device, the Lorentz reciprocity in electro-magnetism should be broken. It can be achieved in three different ways: using magneto-optical material, posing temporal modulation of the material and employing optical nonlinearity. Topological phase transition can be induced by all the above-mentioned effects. Examples for each type will be introduced for topological isolators. Specifically, an optical circulator is essentially a multiport realization of an isolator, which will be discussed in the same classification along with the isolator.

Magneto-optic material breaks the Lorentz reciprocity easily, and has been widely used in nonreciprocal devices<sup>109</sup>. Wong et al.<sup>110</sup> introduced a topological theory for perfect isolation based on metasurface, using magneto-optical material, YIG to build nonreciprocal effects. As shown in Fig. 7c, y-axis is the forward direction for incident light, and green (blue) rods stand for YIG (dielectric material). Parameters including center-to-center displacement  $\mathbf{dr} = (dx, dy)$ , frequency and incident angle of wave form a parameter space, over which the winding number is calculated. As depicted in Fig. 7c, two points at which transmission and reflectance meet 100% are called perfect isolation points. The winding numbers for the two points are +1 and -1, respectively, demonstrating a pair of topological nontrivial isolation points in the parameter space.

Magneto-optic material has also enabled quantum Hall effect in topological photonics and thus brought Lorentz nonreciprocity<sup>12</sup>. By carefully designing the structure, Ma et al. proposed a topological isolator and four-port circulator based on the combination of quantum Hall effect and quantum spin Hall effect<sup>111</sup>. As shown in Fig. 7d, light transmission from two sides is in control of external magnetic field, when the device works as an optical isolator. Based on this complex composition of two types of topological modes, three-port junction and four-port circulator can also be designed.

Despite the great progress of magneto-optic material in nonreciprocal devices, it remains a challenge for on-chip integration<sup>109</sup>, as most materials do not exhibit magneto-optic effect in optical frequency range. For electronic wave propagation, the broken reciprocity by a magnetic field can be derived from a magnetic gauge field. For neutral particles, photons, an effective gauge field can be built to break reciprocity by dynamic modulation<sup>112,113</sup>. Also, topological nontrivial phase can be built from temporal modulation, which brings topological isolator based on dynamic modulation.

Based on temporal modulation over one-dimensional silicon ring resonator, Tomoki et al. introduced a topological phase transition in synthetic dimension<sup>114</sup>. As shown in Fig. 7e,  $J_x$  denotes the tunneling amplitude along the real dimension, and  $J_w$  denotes the coupling in the synthetic dimension. Different modes of the ring resonator are exploited as a synthetic dimension to build 2D quantum Hall effect in structure with periodicity along one dimension in real space. Discrete modes with different frequencies can be viewed as a periodic lattice site if neglecting higher order perturbation. Edge modes at the opposite sites in the real space have opposite orientations in the synthetic dimension. Introduce a high lossy mode in the ring resonators and one creates a sharp boundary in the synthetic dimension. The topological edge modes are prohibited along the synthetic dimension but transmitted along the ring resonator chain. As depicted in Fig. 7f, for light injected with a frequency lower than the lossy mode, only the light from right side can propagate the resonator chain while light from the left side is forbidden.

Zhou et al. introduced nonlinearity in several different models and built optical isolation based on them<sup>115</sup>, which included 1D Su-Schrieffer-Heeger (SSH) model, 2D Haldane model and 2D coupled-ring waveguide. In the 1D SSH model by coupled waveguide array, as shown in Fig. 7g, topological phase transition occurs when the intra-cell coupling coefficient  $\kappa_1$  gets larger than the inter-cell coupling coefficient  $\kappa_2$ . Under open boundary condition, light excitation at the edge diffracts into a superposition of bulk modes for topological trivial phase and localizes at the edge for topological nontrivial phase. The authors took an intercell coupling coefficient dependent on light intensity to introduce nonlinearity. For incident light smaller than a threshold, the system stays in topological trivial state and incident light diffracts into the bulk region. Only if the incident light reaches a threshold where  $\kappa_2 > \kappa_1$ , it transmits through the boundary waveguide. Thus, a nonlinear transmittance is brought by a self-induced topological transition. As shown in Fig. 7g, optical isolation can be achieved by setting different coupling efficiencies,  $\eta_A$  and  $\eta_B$ , at two ports of the edge waveguide. With incident light intensity,  $I$ , the light coupled to the port A and port B from the excitation are  $I\eta_A^2$  and  $I\eta_B^2$ , respectively. Define an operator for the nonlinear transmittance,  $\mathcal{T}$  and the isolation ratio is  $IR = \frac{\mathcal{T}(\eta_A^2 I)}{\mathcal{T}(\eta_B^2 I)}$ . As shown in Fig. 7g, the optical isolation effect in simulation gives a high isolation ratio over if incident light intensity reaches the threshold.

For on-chip integration, it is difficult to apply the magneto-optical effect due to lack of strong light-matter interaction in nanoscale for natural material in the optical frequency range. Building photonic gauge field by dynamic modulation and induce topological transition by nonlinearity can be better ways to design on-chip topological nonreciprocal devices.

**5.3. Topological optical logic devices** The optical logic device is a critical component to realize optical manipulating and all-optical information processing. Unlike the electronic counterpart, the function of optical logic device can be supported by the interference effect of input signals so optical logic devices are essential nanodevices based on phase control. Many optical logic devices have been designed based on photonic crystal, metamaterial, and resonators. They are reported to have compact size and low delay time<sup>118</sup>. But few devices can still have good performance over defects brought by fabrication errors and disorders. This calls for the introduction of topological photonics.

An optical logic device was constructed in valley photonic crystals<sup>99</sup>, which is shown in Fig. 7i. Here, a beam splitter is firstly constructed, and optical logic device is then achieved by controlling reverse behavior of the beam splitter. Place the input signals at port 1 and port 2, define the initial phase difference of the input signals as 0 or  $\pi$ , and the input signals will have destructive interference or constructive interference at the output port. Opposite interference happens at port 3. The above description is the scheme for XOR and OR gate. Other logic gates can also be realized by cascading more geometries.

Optical logic devices can also be constructed with ring resonators<sup>117</sup>. Similar optical interference principle was applied, where two input signals have different initial phase, leading to constructive or destructive interference at the output port. A demonstration of XOR gate is given in Fig. 7j.

**5.4. Opportunities and challenges** The nontrivial topological phase brings robustness to optical switches, optical isolators and optical logic devices. The design of an optical switch requires active control over topological phase transition and special materials possessing high electro-optical coefficient or magneto-optical effect have proven effective. However, this method is not friendly to integration. The topological isolator is a passive device, which is free of external control, but the introduction of nonreciprocity requires magneto-optical material, nonlinearity, or temporal

modulation. More prospective methods are the latter two because of the weak magnetic response of magneto-optical material. Besides, topological logic gates are necessary parts of an optical circuit, while the reported ones are based on interference effects. The propagation of light within these systems is protected by nontrivial topology but the phase accumulation along the propagation path is still sensitive to fabrication defects. It still remains a challenge to develop a better method.

## 6. TOPOLOGICAL QUANTUM INFORMATION PROCESSING

On-chip quantum light information processing can be used to construct quantum computation systems and develop quantum-based algorithms. In recent years, the emerging topological photonics has provided a platform for achieving robust quantum optical chip, which just brings a route to solve the susceptibility of quantum systems. In this section, several typical works about on-chip topological quantum information processing are introduced.

**6.1. Topological quantum information processing devices** In 2018, Barik et al. coupled a quantum emitter with an all-dielectric topological waveguide. Based on the structure shown in Fig. 8a, a strong interface between single quantum emitter and topological edge states were achieved<sup>119</sup>. Their results show that the emission of these modes possesses chirality and the propagation of these modes has robustness against sharp bends.

Quantum correlation between two photons plays an important role in quantum simulation and quantum computation. Blanco-Redondo et al. proposed the first demonstration of topological protection of biphoton states based on a chain of silicon nanowires with the structure shown in Fig. 8b<sup>120</sup>. The designed structure is a one-dimensional array of silicon nanowires, which creates an SSH model by adjusting the gaps between every two adjacent nanowires. A defect was set in the center of the array to act as a topological interface. An intense picosecond pump pulse was injected into the interface and correlated topological defect modes were excited via spontaneous four-wave mixing. The experimental results showed that the correlation was robust to introduced disorders. They also presented the first experimental demonstration of topological protection of entangled biphoton states based on SSH model<sup>121</sup>. The SEM image of the designed structure is shown in Fig. 8c. Most recently, they experimentally proposed the entanglement of photons with different topology, in an array of silicon waveguides<sup>122</sup>. It can be seen that there are three generated modes in the defect of the designed array of silicon waveguides from the left of Fig. 8d. From the right side of Fig. 8d, normalized pump intensity and biphoton probabilities are plotted.

Topologically protected two-photon quantum states was also performed experimentally by Wang et al. on a photonic chip composed of waveguides<sup>123</sup>. They built topological states based on off-diagonal Harper model and realized the system on a waveguide array made of borosilicate glass, which was fabricated with a femtosecond laser direct writing technique. The designed structure is shown in Fig. 8e. By analyzing the quantum correlation of the topological boundary states, a high cross-correlation and a strong violation of Cauchy-Schwarz inequality were realized. Moreover, they also experimentally performed topologically protected polarization quantum entanglement on a similar photonic chip<sup>124</sup>, as shown in Fig. 8f. Their results showed that quantum entanglement can be well preserved when disorder and relative polarization rotation are introduced into the system.

Tambasco et al. also performed quantum interference of single-photon topological states on a light chip<sup>125</sup>. The designed structure is a photonic waveguide array, which implements the off-diagonal Harper model, as

shown in Fig. 8g. This model supports two edge states at the boundaries of the array. By tuning the time-varying Hamiltonian to control the band structure of the device, they implemented a 50:50 beam splitter of topological states. Based on this device, Hong-Ou-Mandel interference was observed with high visibility. The achievement of topological quantum interference is useful for robust linear optical quantum computation.

Squeezed light is a key resource in quantum sensing and quantum information processing. Recently, Ren et al. have performed experimentally the generation of squeezed light on a silica chip<sup>126</sup>. They achieved SSH model on a photonic chip, which is shown in Fig. 8h. With the edge states, they performed topologically protected nonlinear process of four-wave mixing to generate squeezed light.

Chen et al. realized a quantum light circuit based on valley photonic crystals<sup>127</sup>. They designed and fabricated harpoon-shaped beam splitters with topological interfaces. By cascading splitters together, they achieved a quantum photonic circuit, on which Hong-Ou-Mandel interference can be observed. The experimental setup is shown in Fig. 8i.

**6.2. Opportunities and challenges** One of the key features in the application of quantum information system is the quantumness which can be affected by disorders in structures. The introduction of topological photonics makes the protection of quantumness of the systems more reliable<sup>123</sup>. However, there still exist great challenges in the development of topological quantum information processing. Firstly, it is still difficult to expand topological quantum information processing system to higher dimensions, which is meaningful for increasing the information carrying capability of the design system. Secondly, much more explorations are still needed to build topological quantum information networks, which is an important step towards topological quantum photonic chip integration in the future.

## 7. TOPOLOGICAL LIGHT AMPLIFIERS AND SENSORS

Light receiving is a basic step to collect and detect the signals on chip. Light detecting devices receive the optical information from outside and convert the signal supported by the optical integrated net. In this section, topological light detecting devices are introduced, including topological light amplifiers and topological light sensors.

**7.1. Topological light amplifiers** The light amplifier is an important part of light receiving process. Traditional fiber light amplifiers are not very convenient to be integrated on a chip, and semiconductor light amplifiers do not possess high stability. The introduction of topological edge states is expected to help with these problems.

Light amplification is inseparable from the study of non-Hermitian systems. Porras et al. designed a topological amplifier in photonic lattices with dissipative couplings in a non-Hermitian system<sup>128</sup>. Topological protected edge states which govern the response to a coherent drive lead to an exponential amplification effect and an example of an array of coupled photonic cavities is given. This work presents a novel approach to the singular value decomposition (SVD) of the non-Hermitian coupling matrix, which is formally equivalent to the diagonalization of an effective Hamiltonian. The mapping of the SVD of Hamiltonian to an effective Hamiltonian  $\mathcal{H}$  allows the use of the theoretical machinery of topological band theory. The topological band theory can predict the existence of edge states. In the one-dimensional finite size lattice model, the edge singular value decays exponentially with the length of the system  $L$  divided by a typical length,  $\chi$ . The steady-state solution is inversely proportional to the edge singular value according to the SVD of Hamiltonian, which means that the existence of edge states of  $\mathcal{H}$  leads to the amplification of

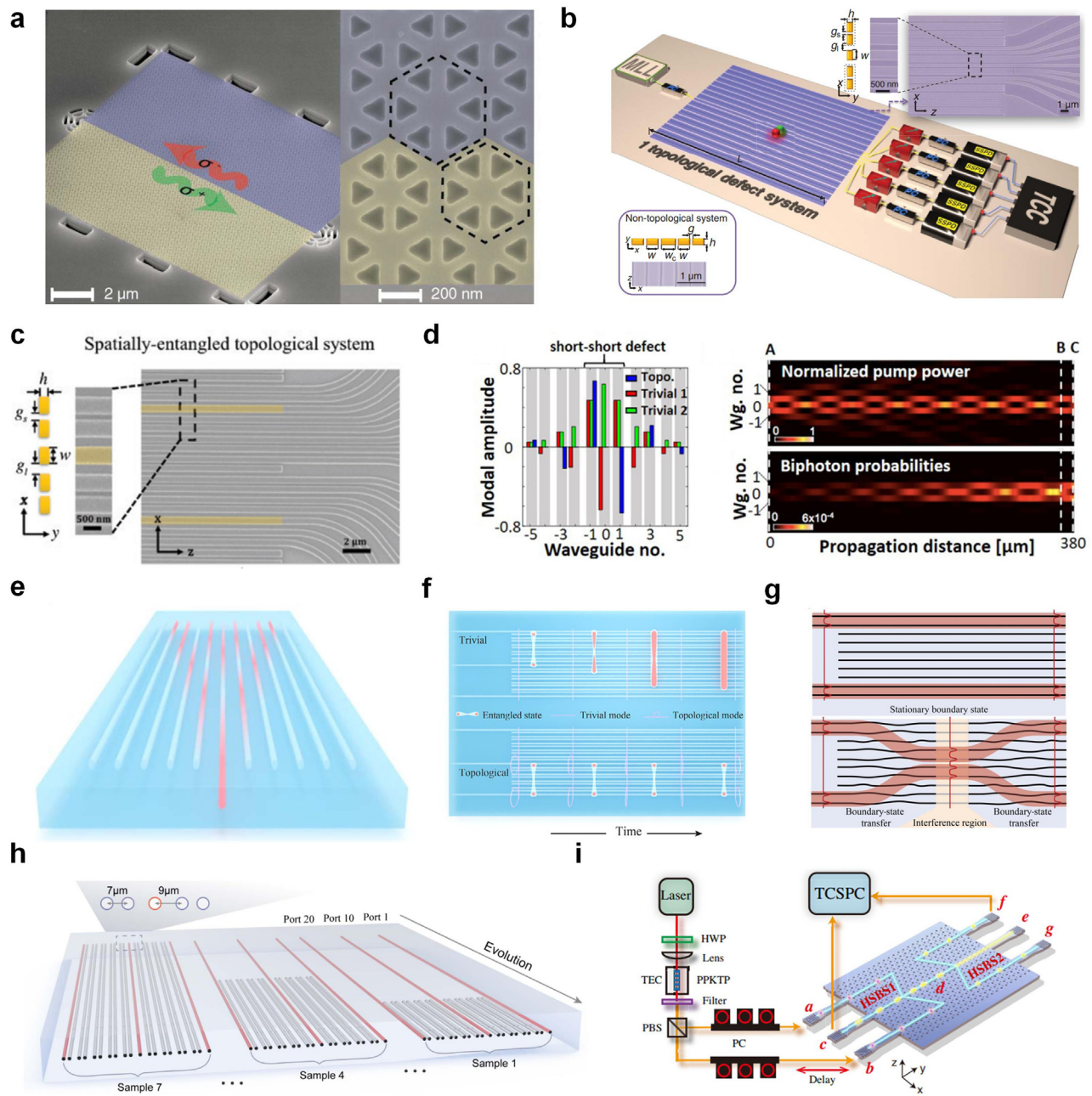


**Fig. 8 | Devices of topological quantum light processing.** **a**, Interface between single quantum emitter and topological edge states. **b**, Achievement of topological projection of biphoton states based on silicon nanowire array<sup>120</sup>. Reprinted with permission from ref.<sup>119,120</sup>. © 2018 American Association for the Advancement of Science. **c**, Experimental demonstration of topologically protected biphoton path entanglement. Reprinted with permission from ref.<sup>121</sup>. © 2019 De Gruyter. **d**, Biphoton entanglement between modes with different topology. Reprinted with permission from ref.<sup>122</sup>. © 2022 American Physical Society. **e**, Achievement of topological protection of two-photon quantum states based on waveguide array. Reprinted with permission from ref.<sup>123</sup>. © 2019 Optical Society of America. **f**, Topologically protected polarization quantum entangled states. Reprinted with permission from ref.<sup>124</sup>. © 2022 Elsevier B.V. **g**, Quantum interference of two single-photon topological boundary states in a photonic waveguide array. Reprinted with permission from ref.<sup>125</sup>. © 2018 American Association for the Advancement of Science. **h**, Achievement of topologically protected squeezed light. Reprinted with permission from ref.<sup>126</sup>. © 2022 Nature Publishing Group. **i**, Topologically protected valley-dependent quantum circuits. Reprinted with permission from ref.<sup>127</sup>. © 2021 American Physical Society.

a coherent drive. Considering an array of cavities with nearest-neighbor dissipative couplings, the effective Hamiltonian in the plane-wave basis will give the edge state wave functions which have an exponential relationship to site number  $N$ . In Fig. 9a, a chain of  $N$  cavities is coupled to an auxiliary chain and the frequency gradient is used to break time-reversal

symmetry. The white circles represent main local photonic modes and the orange circles represent auxiliary fast decaying modes for reservoir engineering. The coupling  $g$  with periodic modulations and collective incoherent pumping from the auxiliary cavities allow dissipative coupling matrix to satisfy topological phases.

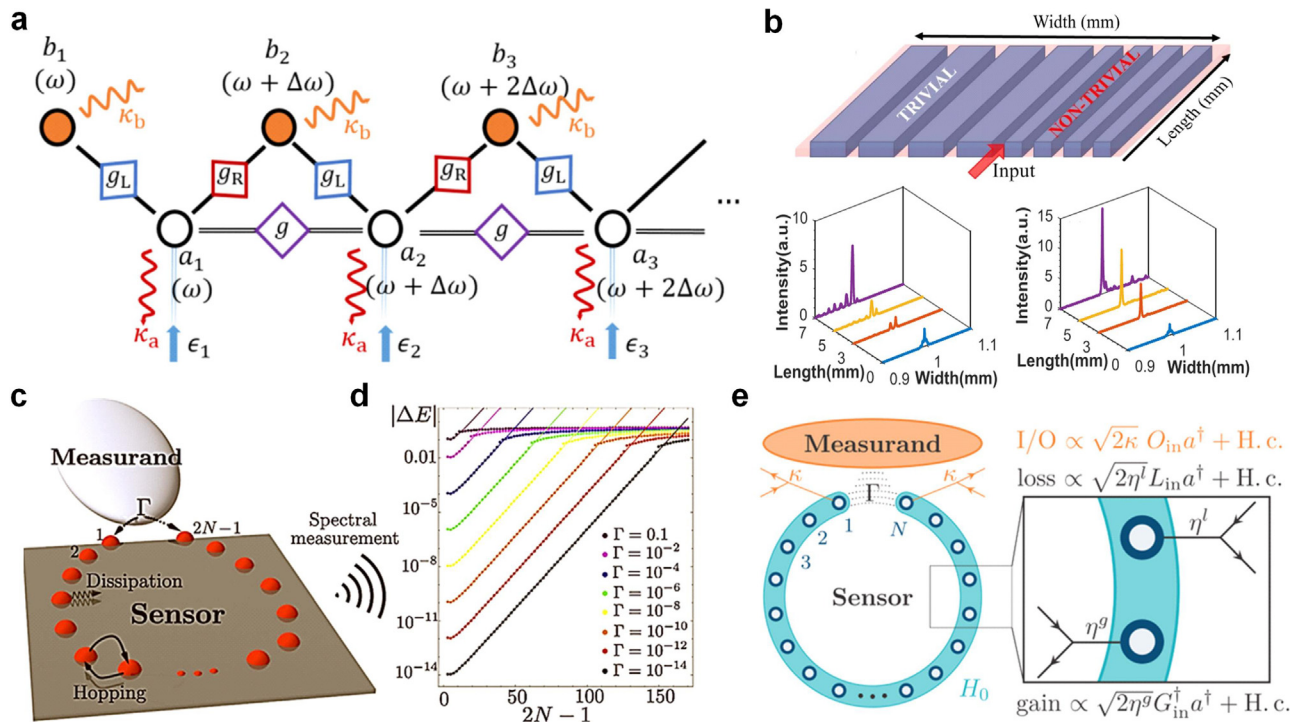


**Fig. 9** | **a**, A physical implementation of the 1D topological amplifier. Reprinted with permission from ref.<sup>128</sup>. © 2019 American Physical Society. **b**, Scheme of topological amplification based on a 1D photonic lattice. Reprinted with permission from ref.<sup>129</sup>. © 2021 Optical Society of America. **c**, Illustration of an NTOS setup which consists of a one-dimensional chain with  $2N - 1$  lattice sites in an open ring geometry<sup>137</sup>. **d**, Exponential scaling of  $|\Delta E|$  with system size  $N$  in the NTOS based on the non-Hermitian topological model for different values of  $\Gamma$ <sup>137</sup>. **e**, Illustration of the QUANTOS setup, which consists of an odd number of bosonic modes in an open ring geometry<sup>140</sup>. Reprinted with permission from ref.<sup>137,140</sup>. © 2020, 2022 American Physical Society.

In another way, light amplification was achieved by combining material gain with topological protection. Ghosh et al. presented a 1D photonic lattice, which realizes topological amplification by Zak phase analysis<sup>129</sup>. The device diagram is shown in the upper panel of Fig. 9b, in which blue part represents high refractive index material and red part low refractive index material. High refractive index waveguides with different width and thickness are of different topological properties described by Zak phases. The lower panel of Fig. 9b shows that uniform gain and loss applied to two refractive-index layers make the intensity of Gaussian beams increase when passing through topological edge states. When only uniform gain is applied to low-refractive-index layers, a high-intensity topological light state could be obtained.

Besides, Ling et al. designed a topological amplifier system by studying Bogoliubov-de Gennes (BdG) systems<sup>130</sup>. Stable bulk states and unstable edge states allow the topological amplifier to work. Thus, they presented a theorem which can determine the stability of a state with energy sufficiently far from zero in a BdG system. This theorem applied to a generalization of a model from Galilo et al.<sup>131</sup> makes a topological amplifier work in BdG system.

There are several topological light amplifiers in theory, however, experimental results are still absent. Amplification is an important step for on-chip integration, which can gather and amplify weak signals. The experimental realization of topological light amplifiers will be beneficial for robust receiving and processing of weak signals.

**7.2. Topological light sensors** Due to the advantages of sensor applications, optical sensors have gained tremendous interest and popularity as promising sensors resulting from their particular properties, for example, high speed and remote sensing ability and fast response<sup>132</sup>.

Recently, a new 1D topological photonic crystal heterostructure mirror has been proposed to realize a hybrid resonance mode due to the robust optical localization at the topological edge area with high sensor abilities and performance<sup>133</sup>. A flexible platform was examined to design a topological photonic sensor that can be used for any type of sensor solely by replacing the interface layers with the sensor materials to resolve the problem of defect mode in reducing the value of transmission and appropriate high sensitivity associated with a large  $Q$ -factor<sup>134</sup>.

Moreover, in non-Hermitian lattice systems with many degrees of freedom, an exceptional spectral sensitivity has recently been found in non-Hermitian topological systems, in which phase transitions driven by slight variations in boundary conditions have been predicted and observed<sup>135,136</sup>. Interestingly, by combining non-Hermitian sensing with the topological matter concept, an enhancement in sensitivity that scales exponentially with system size is promoted to a steady phenomenon independent on fine-tuning<sup>137</sup>. These non-Hermitian topological sensors (NTOSs) rely on the energy shift in the topological edge state mode in response to slight variations in the boundary conditions<sup>137-139</sup> of a chain in the broken ring geometry. Their system relies on effectively coupling the physical quantity to be detected with the boundary conditions of an extended system of  $2N - 1$  lattice sites<sup>139</sup>, for example, by modulating the  $\Gamma$  coupling between the NTOS terminus and the tunneling barrier, which is shown in Fig. 9c and d.

A quantum theory for a quantum non-Hermitian topological sensor (QUANTOS) is also presented<sup>140</sup>. The authors studied the relations between inputs and outputs allied with concrete experimental monitoring schemes such as heterodyne detection. There, the probability density for observing the output  $x$  is parametrically dependent on the all-important

boundary state parameter that couples with the observable detection by QUANTOS, which is shown in Fig. 9e.

**7.3. Opportunities and challenges** Light amplifiers based on topological states provide a new platform to detect light, and their performance is hard to be affected by external environment. In general, topological light amplifiers are still in theoretical design now. Amplification of light in transmission is generally achieved by gain and loss of non-Hermitian systems. The physical implementation of the topological amplifier is presented by introducing a dissipative coupled one-dimensional photonic lattice through non-Hermitian theoretical analysis. However, there are potential problems with the introduction of dissipative coupling on chip probably. Another method of light amplification combining gain medium and topological protection is relatively simple, however, the light amplification dynamics given is only based on a Gaussian beam. In addition, bosonic analog of BdG Hamiltonian is a possible approach for topological amplifiers.

As reviewed above, applying non-Hermitian topological phase in sensors can drastically increase the detecting sensitivity. However, the advantages of topological sensors are currently only demonstrated in theory. More experimental efforts are needed to verify their performances. In addition, there are inevitable noises from environment when detecting signals from outside, it still remains a great challenge about how can topological sensors distinguish target signals from the noises.

## 8. OUTLOOK

Topological photonics has been studied for years since 2008<sup>53</sup>, and various topological protection mechanisms were proposed. The novel phenomena of topological photonic crystals open an exciting prospect for realization of robust on-chip optical devices. The propagation of light in the topological channels builds high robust ways for information processing on optical integrated chips. However, there are still challenges for broad applications of on-chip nanophotonic devices.

In general, the applications of topological photonics in on-chip nanophotonic devices are starting to spurt. However, there still exist challenges on integrated devices minimization, strong robustness and compatibility. Firstly, the requirement of periodic lattices in topological photonic crystals leads to a relatively big size of topological photonic devices. Although there is a report about topological corner states based on aperiodic lattices<sup>141</sup>, it is still based on modulation of periodic lattices. Secondly, the robustness of topological photonic crystals is currently limited to imperfection with strength compared with bandgap. Superior robust topological devices, which can work under extremely adverse conditions, are still needed. Thirdly, existing topological nanophotonic devices are based on different topological protection mechanisms. Some of them need external magnetic field, while some others need broken spatial inversion symmetry without magnetic field. Different schemes use different materials and are suitable for different kinds of devices. The variety of topological protection mechanisms may face the problems of compatibility when these topological nanophotonic devices are integrated together.

The field of topological photonics is still developing and big problems call for great methods. Below, we give an outlook on some possible development directions of on-chip topological nanophotonic devices, which will possibly provide a view of the trend in this field.

**8.1. Non-Hermitian on-chip topological nanophotonic devices** Non-Hermitian systems, which have rich physics beyond its Hermitian counterpart, have attracted extensive interest from scholars at home and abroad recently. It is necessary to explore non-Hermitian topological

states due to the fact that the real world is composed of open systems with non-Hermiticity instead of Hermitian systems, and the novel nature of non-Hermitian systems opens up many possibilities for device design. Recently, several works have been proposed to achieve topological devices in the non-Hermitian system. Non-Hermitian control was used to steer topological light propagation along the gain-loss interface of a topological micro-ring photonic lattices<sup>43,142</sup>. Non-Hermitian topological sensors were designed in 2020, the sensitivity of boundary conditions grows exponentially with small changes in the size of devices<sup>137</sup>.

It also faces great challenges due to the complexity of non-Hermitian systems, especially the non-validity of traditional bulk-boundary corresponding relationship, which means the topological properties need to be redefined. There is still rich physics in non-Hermitian system to be explored. For example, recently, the point-gap topology corresponding to non-Hermitian skin effect was realized firstly based on photonic crystals on chip<sup>143</sup>. The point-gap topology was characterized by the winding number corresponding to the closed loop formed in the complex frequency plane.

**8.2. Non-Abelian on-chip topological nanophotonic devices** Non-Abelian gauge field was introduced to explain the strong interaction by Yang and Mills firstly<sup>144</sup>. Later, non-Abelian Aharonov-Bohm effect<sup>145</sup> and non-Abelian anyons and statistics<sup>146</sup> were achieved in classical wave system. Roughly speaking, non-Abelian property means that transformations which are performed in different orders or paths are not equivalent, where the commutative law is not satisfied. It involves the dynamic evolution of different states. Specifically, the non-Abelian phenomenon is special in traversing through band degeneracies, whereas the operator on the non-degenerate path is always Abelian.

Non-Abelian topological devices on the chip are expected to be implemented in one-dimensional twisted waveguide arrays or two-dimensional photonic crystals on a chip. Considering waveguide arrays of a certain length in the z-direction, and the waveguide is twisted in the x-y plane along the z-direction to regulate the coupling between waveguide arrays. When the order of the evolution path is changed, the initial state is transformed into different final states, which show non-Abelian character. The optical mode conversion is realized by designing the distribution of eigenstates between different twisted waveguides. Non-Abelian topological braiding on a chip is also considered as a promising way to realize topological optical quantum computing. However, it is difficult to design topological protection based on the conversion.

**8.3. On-chip topological nanophotonic devices based on metasurface** Metamaterials are artificial materials that exhibit extraordinary physical properties not found in nature. Metasurfaces, the thin film of two-dimensional equivalent of metamaterials, are periodic arrays of subwavelength engineered inclusions that can locally manipulate and enhance wave-matter interactions<sup>147</sup>. In recent years, topological photonic theories such as optical vortices with different topological charges<sup>110,148</sup>, topological corner state<sup>149</sup>, topological  $Z_2$  phase<sup>150</sup> have been verified based on metasurface materials. At the same time, various applications such as topological polariton generations<sup>150,151</sup>, topological invariant measurement<sup>152</sup>, perfect isolators<sup>110</sup> and nonlinear effect enhancement<sup>153</sup> are realized with metamaterials. Metasurface, different from the three-dimensional metamaterials, can be used to provide a chip platform as a thin film and maintain certain unique properties of metamaterials through artificial designing. Metasurface may convert the interesting topological phenomenon from space to chip.

**8.4. On-chip topological nanophotonic devices based on intelligent algorithms** Traditional design methods of topological nanophotonic devices are mostly based on mature physical models. Topological nanophotonic devices can be designed by tuning the parameters under the guidance of physical rules. Actually, the tuning process can be complemented by intelligent algorithms to get nanophotonic devices with excellent performances, as long as the target function can be abstracted out from the design question<sup>154,155</sup>. By introducing intelligent algorithms into the design of topological nanophotonic devices, more complicated structures with greater design space can be achieved. For example, Yuan et al. designed topological wavelength router with an intelligent algorithm<sup>96</sup>. Christiansen et al. designed topological nanophotonic waveguides on dielectric material plate using density-based topology optimization<sup>156</sup>. Chen et al. designed high order topological photonic insulator based on an intelligent topology optimization approach<sup>157,158</sup>. With the designed topological insulators, topological waveguides and cavities can be constructed.

It should be pointed that the ‘topology’ in topology optimization has different meanings with the ‘topology’ in topological insulator. The topological nanophotonic devices designed with topology optimization are of freeform structures, which could broaden the view of the design of topological nanophotonic devices.

**8.5. Multiple functional topological nanophotonic integration** It can be seen that there are various design schemes of topological nanophotonic devices. Different schemes are suitable to design several specific kinds of topological devices. However, to achieve a multiple functional topological nanophotonic integrated chip, it is necessary to consider carefully the compatibility of these different schemes. It is essential to propose a kind of design framework that could include all these different topological nanophotonic devices, which is challenging but still attractive. To achieve this, more theoretical and experimental efforts are needed. All the physical mechanisms introduced and commented in this review can be used as alternatives for constructing topological photonic states. Meanwhile, intelligent algorithms, such as various optimization algorithms, deep-learning methods, can be used to design multiple functional topological nanophotonic devices on one chip to obtain the best performances with novel structures predicted<sup>159</sup>.

## 9. SUMMARY

To sum up, the on-chip topological nanophotonic devices were reviewed from the aspects of chip functions, physical mechanisms, design and fabrication methods, integration, etc. Topological photonic states provide a robust and promising platform for the study of nanophotonic devices and the next-generation photonic chip. The background, development, opportunities and challenges, as well as the outlooks, were given for different on-chip topological nanophotonic devices in each section. The introduction of topological photonics in on-chip nanophotonic devices will accelerate the development of robust light information processing. Future development of this exciting field calls for new concepts in photonic chips, improved fabrication technology, novel materials and deep understanding about the underneath physical mechanisms.

## REFERENCES

- Thouless, D. J., Kohmoto, M., Nightingale, M. P. & den Nijs, M. Quantized Hall conductance in a two-dimensional periodic potential. *Phys. Rev. Lett.* **49**, 405 (1982). <https://doi.org/10.1103/PhysRevLett.49.405>.
- Kohmoto, M. Topological invariant and the quantization of the Hall conductance. *Ann. Phys. (N. Y.)* **160**, 343–354 (1985). [https://doi.org/10.1016/0003-4916\(85\)90148-4](https://doi.org/10.1016/0003-4916(85)90148-4).
- Klitzing, K. v., Dorda, G. & Pepper, M. New method for high-accuracy determination of the fine-structure constant based on quantized Hall resistance. *Phys. Rev. Lett.* **45**, 494–497 (1980). <https://doi.org/10.1103/PhysRevLett.45.494>.
- Lu, L., Joannopoulos, J. D. & Soljačić, M. Topological photonics. *Nat. Photonics* **8**, 821–829 (2014). <https://doi.org/10.1038/nphoton.2014.248>.
- Khanikaev, A. B. & Shvets, G. Two-dimensional topological photonics. *Nat. Photonics* **11**, 763–773 (2017). <https://doi.org/10.1038/s41566-017-0048-5>.
- Ozawa, T. et al. Topological photonics. *Rev. Mod. Phys.* **91**, 015006 (2019). <https://doi.org/10.1103/RevModPhys.91.015006>.
- Haldane, F. D. M. & Raghu, S. Possible realization of directional optical waveguides in photonic crystals with broken time-reversal symmetry. *Phys. Rev. Lett.* **100**, 013904 (2008). <https://doi.org/10.1103/PhysRevLett.100.013904>.
- Wang, Z., Chong, Y. D., Joannopoulos, J. D. & Soljačić, M. Reflection-free one-way edge modes in a gyromagnetic photonic crystal. *Phys. Rev. Lett.* **100**, 013905 (2008). <https://doi.org/10.1103/PhysRevLett.100.013905>.
- Wang, Z., Chong, Y., Joannopoulos, J. D. & Soljačić, M. Observation of unidirectional backscattering-immune topological electromagnetic states. *Nature* **461**, 772–775 (2009). <https://doi.org/10.1038/nature08293>.
- Ota, Y. et al. Active topological photonics. *Nanophotonics* **9**, 547–567 (2020). <https://doi.org/10.1515/nanoph-2019-0376>.
- Wu, Y. et al. Applications of topological photonics in integrated photonic devices. *Adv. Opt. Mater.* **5**, 1700357 (2017). <https://doi.org/10.1002/adom.201700357>.
- Smirnova, D., Leykam, D., Chong, Y. & Kivshar, Y. Nonlinear topological photonics. *Appl. Phys. Rev.* **7**, 021306 (2020). <https://doi.org/10.1063/1.5142397>.
- Yan, Q. et al. Quantum topological photonics. *Adv. Opt. Mater.* **9**, 2001739 (2021). <https://doi.org/10.1002/adom.202001739>.
- Segev, M. & Bandres, M. A. Topological photonics: Where do we go from here? *Nanophotonics* **10**, 425–434 (2021). <https://doi.org/10.1515/nanoph-2020-0441>.
- Wang, X., Zhao, W., Zhang, H., Elshahat, S. & Lu, C. Magnetic-optic effect-based topological state: realization and application. *Front. Mater.* **8**, 816877 (2022). <https://doi.org/10.3389/fmats.2021.816877>.
- Blanco-Redondo, A. Topological nanophotonics: toward robust quantum circuits. *Proc. IEEE* **108**, 837–849 (2019). <https://doi.org/10.1109/JPROC.2019.2939987>.
- Rider, M. S. et al. A perspective on topological nanophotonics: current status and future challenges. *J. Appl. Phys.* **125**, 120901 (2019). <https://doi.org/10.1063/1.5086433>.
- Price, H. et al. Roadmap on topological photonics. *J. Phys. Photonics* **4**, 032501 (2022). <https://doi.org/10.1088/2515-7647/ac4ee4>.
- Yang, Y., Poo, Y., Wu, R., Gu, Y. & Chen, P. Experimental demonstration of one-way slow wave in waveguide involving gyromagnetic photonic crystals. *Appl. Phys. Lett.* **102**, 231113 (2013). <https://doi.org/10.1063/1.4809956>.
- Blanco-Redondo, A. et al. Topological optical waveguiding in silicon and the transition between topological and trivial defect states. *Phys. Rev. Lett.* **116**, 163901 (2016). <https://doi.org/10.1103/PhysRevLett.116.163901>.
- Markov, I. L. Limits on fundamental limits to computation. *Nature* **512**, 147–154 (2014). <https://doi.org/10.1038/nature13570>.
- Sun, C. et al. Single-chip microprocessor that communicates directly using light. *Nature* **528**, 534–538 (2015). <https://doi.org/10.1038/nature16454>.
- Kok, P. et al. Linear optical quantum computing with photonic qubits. *Rev. Mod. Phys.* **79**, 135–174 (2007). <https://doi.org/10.1103/RevModPhys.79.135>.
- Ji, Y. et al. Prospects and research issues in multi-dimensional all optical networks. *Sci. China Inf. Sci.* **59**, 101301 (2016). <https://doi.org/10.1007/s11432-016-0324-7>.
- Caulfield, H. J. & Dolev, S. Why future supercomputing requires optics. *Nat. Photonics* **4**, 261–263 (2010). <https://doi.org/10.1038/nphoton.2010.94>.
- Liu, J.-W. et al. Valley photonic crystals. *Adv. Phys.: X* **6**, 1905546 (2021). <https://doi.org/10.1080/23746149.2021.1905546>.
- Tang, G. et al. Topological photonic crystals: physics, designs, and applications. *Laser Photonics Rev.* **16**, 2100300 (2022). <https://doi.org/10.1002/lpor.202100300>.
- Bahari, B. et al. Nonreciprocal lasing in topological cavities of arbitrary geometries. *Science* **358**, 636–640 (2017). <https://doi.org/10.1126/science.aao4551>.
- Bandres, M. A. Khajavikhan, M. et al. Topological insulator laser: experiments. *Science* **359**, eaar4005 (2018). <https://doi.org/10.1126/science.aar4005>.
- Harari, G. et al. Topological insulator laser: theory. *Science* **359**, eaar4003 (2018). <https://doi.org/10.1126/science.aar4003>.
- Zeng, Y. et al. Electrically pumped topological laser with valley edge modes. *Nature* **578**, 246–250 (2020). <https://doi.org/10.1038/s41586-020-1981-x>.
- Shao, Z.-K. et al. A high-performance topological bulk laser based on band-inversion-induced reflection. *Nat. Nanotechnol.* **15**, 67–72 (2020). <https://doi.org/10.1038/s41565-019-0584-x>.
- Yang, Z.-Q., Shao, Z.-K., Chen, H.-Z., Mao, X.-R. & Ma, R.-M. Spin-momentum-locked edge mode for topological vortex lasing. *Phys. Rev. Lett.* **125**, 013903 (2020). <https://doi.org/10.1103/PhysRevLett.125.013903>.
- Gao, X. et al. Dirac-vortex topological cavities. *Nat. Nanotechnol.* **15**, 1012–1018 (2020). <https://doi.org/10.1038/s41565-020-0773-7>.

35. Yang, L., Li, G., Gao, X. & Lu, L. Topological-cavity surface-emitting laser. *Nat. Photonics* **16**, 279–283 (2022). <https://doi.org/10.1038/s41566-022-00972-6>.
36. Zhang, W. et al. Low-threshold topological nanolasers based on the second-order corner state. *Light Sci. Appl.* **9**, 1–6 (2020). <https://doi.org/10.1038/s41377-020-00352-1>.
37. Contractor, R. et al. Scalable single-mode surface emitting laser via open-Dirac singularities. *Nature* **608**, 692–698 (2022). <https://doi.org/10.1038/s41586-022-05021-4>.
38. Zhang, H., Zheng, Y., Yu, Z.-M., Hu, X. & Lu, C. Topological hybrid nanocavity for coupling phase transition. *J. Opt.* **23**, 124002 (2021). <https://doi.org/10.1088/2040-8986/ac2fd2>.
39. Rider, M. S. et al. Advances and prospects in topological nanoparticle photonics. *ACS Photonics* **9**, 1483–1499 (2022). <https://doi.org/10.1021/acsp Photonics.1c01874>.
40. Mittal, S., Goldschmidt, E. A. & Hafezi, M. A topological source of quantum light. *Nature* **561**, 502–506 (2018). <https://doi.org/10.1038/s41586-018-0478-3>.
41. Dai, T. et al. Topologically protected quantum entanglement emitters. *Nat. Photonics* **16**, 248–257 (2022). <https://doi.org/10.1038/s41566-021-00944-2>.
42. Mittal, S., Orre, V. V., Goldschmidt, E. A. & Hafezi, M. Tunable quantum interference using a topological source of indistinguishable photon pairs. *Nat. Photonics* **15**, 542–548 (2021). <https://doi.org/10.1038/s41566-021-00810-1>.
43. Ao, Y. et al. Topological phase transition in the non-Hermitian coupled resonator array. *Phys. Rev. Lett.* **125**, 013902 (2020). <https://doi.org/10.1103/PhysRevLett.125.013902>.
44. Chen, W.-J. et al. Experimental realization of photonic topological insulator in a uniaxial metacrystal waveguide. *Nat. Commun.* **5**, 5782 (2014). <https://doi.org/10.1038/ncomms6782>.
45. Skirlo, S. A. et al. Experimental observation of large Chern numbers in photonic crystals. *Phys. Rev. Lett.* **115**, 253901 (2015). <https://doi.org/10.1103/PhysRevLett.115.253901>.
46. Yves, S. et al. Crystalline metamaterials for topological properties at sub-wavelength scales. *Nat. Commun.* **8**, 16023 (2017). <https://doi.org/10.1038/ncomms16023>.
47. Wu, X. et al. Direct observation of valley-polarized topological edge states in designer surface plasmon crystals. *Nat. Commun.* **8**, 1304 (2017). <https://doi.org/10.1038/s41467-017-01515-2>.
48. Gao, F. et al. Topologically protected refraction of robust kink states in valley photonic crystals. *Nat. Phys.* **14**, 6 (2018). <https://doi.org/10.1038/nphys4304>.
49. Rechtsman, M. C. et al. Photonic Floquet topological insulators. *Nature* **496**, 196–200 (2013). <https://doi.org/10.1038/nature12066>.
50. Hafezi, M., Mittal, S., Fan, J., Migdall, A. & Taylor, J. M. Imaging topological edge states in silicon photonics. *Nat. Photonics* **7**, 1001–1005 (2013). <https://doi.org/10.1038/nphoton.2013.274>.
51. Mittal, S. et al. Topologically robust transport of photons in a synthetic gauge field. *Phys. Rev. Lett.* **113**, 087403 (2014). <https://doi.org/10.1103/PhysRevLett.113.087403>.
52. Noh, J., Huang, S., Chen, K. P. & Rechtsman, M. C. Observation of photonic topological valley Hall edge states. *Phys. Rev. Lett.* **120**, 063902 (2018). <https://doi.org/10.1103/PhysRevLett.120.063902>.
53. Raghu, S. & Haldane, F. D. M. Analogs of quantum-Hall-effect edge states in photonic crystals. *Phys. Rev. A* **78**, 033834 (2008). <https://doi.org/10.1103/PhysRevA.78.033834>.
54. Fu, J.-X., Lian, J., Liu, R.-J., Gan, L. & Li, Z.-Y. Unidirectional channel-drop filter by one-way gyromagnetic photonic crystal waveguides. *Appl. Phys. Lett.* **98**, 211104 (2011). <https://doi.org/10.1063/1.3593027>.
55. Lian, J., Fu, J.-X., Gan, L. & Li, Z.-Y. Robust and disorder-immune magnetically tunable one-way waveguides in a gyromagnetic photonic crystal. *Phys. Rev. B* **85**, 125108 (2012). <https://doi.org/10.1103/PhysRevB.85.125108>.
56. Mansha, S. & Chong, Y. D. Robust edge states in amorphous gyromagnetic photonic lattices. *Phys. Rev. B* **96**, 121405 (2017). <https://doi.org/10.1103/PhysRevB.96.121405>.
57. Onbasli, M. C. et al. Optical and magneto-optical behavior of Cerium Yttrium Iron Garnet thin films at wavelengths of 200–1770 nm. *Sci. Rep.* **6**, 23640 (2016). <https://doi.org/10.1038/srep23640>.
58. Kane, C. L. & Mele, E. J. Quantum spin Hall effect in graphene. *Phys. Rev. Lett.* **95**, 226801 (2005). <https://doi.org/10.1103/PhysRevLett.95.226801>.
59. Hafezi, M., Demler, E. A., Lukin, M. D. & Taylor, J. M. Robust optical delay lines with topological protection. *Nat. Phys.* **7**, 907–912 (2011). <https://doi.org/10.1038/nphys2063>.
60. Liang, G. Q. & Chong, Y. D. Optical resonator analog of a two-dimensional topological insulator. *Phys. Rev. Lett.* **110**, 203904 (2013). <https://doi.org/10.1103/PhysRevLett.110.203904>.
61. Khanikaev, A. B. et al. Photonic topological insulators. *Nat. Mater.* **12**, 233–239 (2013). <https://doi.org/10.1038/nmat3520>.
62. Yang, Y. et al. Visualization of a unidirectional electromagnetic waveguide using topological photonic crystals made of dielectric materials. *Phys. Rev. Lett.* **120**, 217401 (2018). <https://doi.org/10.1103/PhysRevLett.120.217401>.
63. Barik, S., Miyake, H., DeGottardi, W., Waks, E. & Hafezi, M. Two-dimensionally confined topological edge states in photonic crystals. *New J. Phys.* **18**, 113013 (2016). <https://doi.org/10.1088/1367-2630/18/11/113013>.
64. Gao, Z. et al. Valley surface-wave photonic crystal and its bulk/edge transport. *Phys. Rev. B* **96**, 201402 (2017). <https://doi.org/10.1103/PhysRevB.96.201402>.
65. Wu, L.-H. & Hu, X. Scheme for achieving a topological photonic crystal by using dielectric material. *Phys. Rev. Lett.* **114**, 223901 (2015). <https://doi.org/10.1103/PhysRevLett.114.223901>.
66. Ma, T. & Shvets, G. All-Si valley-Hall photonic topological insulator. *New J. Phys.* **18**, 025012 (2016). <https://doi.org/10.1088/1367-2630/18/2/025012>.
67. He, X.-T. et al. A silicon-on-insulator slab for topological valley transport. *Nat. Commun.* **10**, 1–9 (2019). <https://doi.org/10.1038/s41467-019-08881-z>.
68. Mock, A., Lu, L. & O'Brien, J. Space group theory and Fourier space analysis of two-dimensional photonic crystal waveguides. *Phys. Rev. B* **81**, 155115 (2010). <https://doi.org/10.1103/PhysRevB.81.155115>.
69. Mahmoodian, S., Prindal-Nielsen, K., Söllner, I., Stobbe, S. & Lodahl, P. Engineering chiral light-matter interaction in photonic crystal waveguides with slow light. *Opt. Mater. Express* **7**, 43–51 (2017). <https://doi.org/10.1364/OME.7.000043>.
70. Arregui, G., Gomis-Bresco, J., Sotomayor-Torres, C. M. & Garcia, P. D. Quantifying the robustness of topological slow light. *Phys. Rev. Lett.* **126**, 027403 (2021). <https://doi.org/10.1103/PhysRevLett.126.027403>.
71. Ouyang, C. et al. Slow light with low group-velocity dispersion at the edge of photonic graphene. *Phys. Rev. A* **84**, 015801 (2011). <https://doi.org/10.1103/PhysRevA.84.015801>.
72. Yablonoich, E. One-way road for light. *Nature* **461**, 744–745 (2009). <https://doi.org/10.1038/461744a>.
73. Lindner, N. H. Floquet topological insulator in semiconductor quantum wells. *Nat. Phys.* **7**, 6 (2011). <https://doi.org/10.1038/nphys1926>.
74. Gu, Z., Fertig, H. A., Arova, D. P. & Auerbach, A. Floquet spectrum and transport through an irradiated graphene ribbon. *Phys. Rev. Lett.* **107**, 216601 (2011). <https://doi.org/10.1103/PhysRevLett.107.216601>.
75. Lin, Q., Xiao, M., Yuan, L. & Fan, S. Photonic Weyl point in a two-dimensional resonator lattice with a synthetic frequency dimension. *Nat. Commun.* **7**, 13731 (2016). <https://doi.org/10.1038/ncomms13731>.
76. Lin, Q., Sun, X.-Q., Xiao, M., Zhang, S.-C. & Fan, S. A three-dimensional photonic topological insulator using a two-dimensional ring resonator lattice with a synthetic frequency dimension. *Sci. Adv.* **4**, eaat2774 (2018). <https://doi.org/10.1126/sciadv.aat2774>.
77. Maczewsky, L. J., Zeuner, J. M., Nolte, S. & Szameit, A. Observation of photonic anomalous Floquet topological insulators. *Nat. Commun.* **8**, 13756 (2017). <https://doi.org/10.1038/ncomms13756>.
78. Mukherjee, S. et al. Experimental observation of anomalous topological edge modes in a slowly driven photonic lattice. *Nat. Commun.* **8**, 13918 (2017). <https://doi.org/10.1038/ncomms13918>.
79. Pasek, M. & Chong, Y. D. Network models of photonic Floquet topological insulators. *Phys. Rev. B* **89**, 075113 (2014). <https://doi.org/10.1103/PhysRevB.89.075113>.
80. Rudner, M. S., Lindner, N. H., Berg, E. & Levin, M. Anomalous edge states and the bulk-edge correspondence for periodically driven two-dimensional systems. *Phys. Rev. X* **3**, 031005 (2013). <https://doi.org/10.1103/PhysRevX.3.031005>.
81. Lu, C., Wang, C., Xiao, M., Zhang, Z. Q. & Chan, C. T. Topological rainbow concentrator based on synthetic dimension. *Phys. Rev. Lett.* **126**, 113902 (2021). <https://doi.org/10.1103/PhysRevLett.126.113902>.
82. Lu, C. et al. On-chip nanophotonic topological rainbow. *Nat. Commun.* **13**, 2586 (2022). <https://doi.org/10.1038/s41467-022-30276-w>.
83. Zhang, H. et al. Topological rainbow based on graded topological photonic crystals. *Opt. Lett.* **46**, 1237–1240 (2021). <https://doi.org/10.1364/OL.419271>.
84. Elshahat, S., Esmail, M. S. M., Yuan, H., Feng, S. & Lu, C. Broadband multiple topological rainbows. *Ann. Phys. (Berl.)* **534**, 2200137 (2022). <https://doi.org/10.1002/andp.202200137>.
85. Li, M. X., Wang, Y. K., Lu, M. J. & Sang, T. Dual-mode of topological rainbow in gradual photonic heterostructures. *J. Phys. D: Appl. Phys.* **55**, 095103 (2022). <https://doi.org/10.1088/1361-6463/ac37df>.
86. Mao, Y., Li, Z., Hu, W., Dai, X. & Xiang, Y. Topological slow light rainbow trapping and releasing based on gradient valley photonic crystal. *J. Light. Technol.* **40**, 5152–5156 (2022). <https://doi.org/10.1109/JLT.2022.3171289>.
87. Liang, L. et al. Rainbow trapping based on higher-order topological corner modes. *Opt. Lett.* **47**, 1454–1457 (2022). <https://doi.org/10.1364/OL.451770>.
88. Elshahat, S. & Lu, C. Bidirectional rainbow trapping in 1-D chirped topological photonic crystal. *Front. Phys.* **10**, 831203 (2022). <https://doi.org/10.3389/fphy.2022.831203>.
89. Mao, Y., Hu, W., Li, Z., Dai, X. & Xiang, Y. Engineering rainbow trapping and releasing in valley photonic crystal with electro-optical material. *J. Opt. Soc. Am. B* **39**, 1241–1246 (2022). <https://doi.org/10.1364/JOSAB.452642>.
90. Xu, Q., Schmidt, B., Shakya, J. & Lipson, M. Cascaded silicon micro-ring modulators for WDM optical interconnection. *Opt. Express* **14**, 9431–9436 (2006). <https://doi.org/10.1364/OE.14.009431>.

91. Skirlo, S. A., Lu, L. & Soljačić, M. Multimode one-way waveguides of large chern numbers. *Phys. Rev. Lett.* **113**, 113904 (2014). <https://doi.org/10.1103/PhysRevLett.113.113904>.
92. He, C. et al. Tunable one-way cross-waveguide splitter based on gyromagnetic photonic crystal. *Appl. Phys. Lett.* **96**, 111111 (2010). <https://doi.org/10.1063/1.3358386>.
93. Cheng, X. et al. Robust reconfigurable electromagnetic pathways within a photonic topological insulator. *Nat. Mater.* **15**, 542–548 (2016). <https://doi.org/10.1038/nmat4573>.
94. Chen, X.-D., Deng, Z.-L., Chen, W.-J., Wang, J.-R. & Dong, J.-W. Manipulating pseudospin-polarized state of light in dispersion-immune photonic topological metacrystals. *Phys. Rev. B* **92**, 014210 (2015). <https://doi.org/10.1103/PhysRevB.92.014210>.
95. Ma, J., Xi, X. & Sun, X. Topological photonic integrated circuits based on valley kink states. *Laser Photonics Rev.* **13**, 1900087 (2019). <https://doi.org/10.1002/lpor.201900087>.
96. Yuan, H. et al. Topological nanophotonic wavelength router based on topology optimization. *Micromachines* **12**, 1506 (2021). <https://doi.org/10.3390/mi12121506>.
97. Wang, H. et al. Asymmetric topological valley edge states on silicon-on-insulator platform. *Laser Photonics Rev.* **16**, 2100631 (2022). <https://doi.org/10.1002/lpor.202100631>.
98. Hong, Y.-L. et al. Direct observation of terahertz topological valley transport. *Opt. Express* **30**, 14839 (2022). <https://doi.org/10.1364/OE.454750>.
99. He, L., Ji, H. Y., Wang, Y. J. & Zhang, X. D. Topologically protected beam splitters and logic gates based on two-dimensional silicon photonic crystal slabs. *Opt. Express* **28**, 34015–34023 (2020). <https://doi.org/10.1364/OE.409265>.
100. Kang, Y., Ni, X., Cheng, X., Khanikaev, A. B. & Genack, A. Z. Pseudo-spin-valley coupled edge states in a photonic topological insulator. *Nat. Commun.* **9**, 3029 (2018). <https://doi.org/10.1038/s41467-018-05408-w>.
101. Han, N., Liu, J., Gao, Y., Zhou, K. & Liu, S. Robust gapped surface states and filtering effect in a photonic topological gyroelectromagnetic metamaterial. *Phys. Rev. B* **104**, 205403 (2021). <https://doi.org/10.1103/PhysRevB.104.205403>.
102. Gu, L. et al. A topological photonic ring-resonator for on-chip channel filters. *J. Light. Technol.* **39**, 5069–5073 (2021). <https://doi.org/10.1109/JLT.2021.3082558>.
103. Asadchy, V. S., Díaz-Rubio, A. & Tretyakov, S. A. Bianisotropic metasurfaces: physics and applications. *Nanophotonics* **7**, 1069–1094 (2018). <https://doi.org/10.1515/nanoph-2017-0132>.
104. Qi, H. et al. All-optical switch based on novel physics effects. *J. Appl. Phys.* **129**, 210906 (2021). <https://doi.org/10.1063/5.0048878>.
105. Luo, X.-W., Zhang, C., Guo, G.-C. & Zhou, Z.-W. Topological photonic orbital-angular-momentum switch. *Phys. Rev. A* **97**, 043841 (2018). <https://doi.org/10.1103/PhysRevA.97.043841>.
106. Wu, Y., Hu, X. & Gong, Q. Reconfigurable topological states in valley photonic crystals. *Phys. Rev. Mater.* **2**, 122201 (2018). <https://doi.org/10.1103/PhysRevMaterials.2.122201>.
107. Pirie, H., Sadhuka, S., Wang, J., Andrei, R. & Hoffman, J. E. Topological phononic logic. *Phys. Rev. Lett.* **128**, 015501 (2022). <https://doi.org/10.1103/PhysRevLett.128.015501>.
108. Seif, A. & Hafezi, M. Broadband optomechanical non-reciprocity. *Nat. Photonics* **12**, 60–61 (2018). <https://doi.org/10.1038/s41566-018-0091-x>.
109. Fan, S., Shi, Y. & Lin, Q. Nonreciprocal photonics without magneto-optics. *IEEE Antennas Wirel. Propag. Lett.* **17**, 1948–1952 (2018). <https://doi.org/10.1109/lawp.2018.2856258>.
110. Wong, W. C., Wang, W., Yau, W. T. & Fung, K. H. Topological theory for perfect metasurface isolators. *Phys. Rev. B* **101**, 121405 (2020). <https://doi.org/10.1103/PhysRevB.101.121405>.
111. Ma, S. et al. Topologically protected photonic modes in composite quantum Hall/quantum spin Hall waveguides. *Phys. Rev. B* **100**, 085118 (2019). <https://doi.org/10.1103/PhysRevB.100.085118>.
112. Fang, K., Yu, Z. & Fan, S. Realizing effective magnetic field for photons by controlling the phase of dynamic modulation. *Nat. Photonics* **6**, 782–787 (2012). <https://doi.org/10.1038/nphoton.2012.236>.
113. Fang, K., Yu, Z. & Fan, S. Photonic Aharonov-Bohm effect based on dynamic modulation. *Phys. Rev. Lett.* **108**, 153901 (2012). <https://doi.org/10.1103/PhysRevLett.108.153901>.
114. Ozawa, T., Price, H. M., Goldman, N., Zilberberg, O. & Carusotto, I. Synthetic dimensions in integrated photonics: from optical isolation to four-dimensional quantum Hall physics. *Phys. Rev. A* **93**, 043827 (2016). <https://doi.org/10.1103/PhysRevA.93.043827>.
115. Zhou, X., Wang, Y., Leykam, D. & Chong, Y. D. Optical isolation with nonlinear topological photonics. *New J. Phys.* **19**, 095002 (2017). <https://doi.org/10.1088/1367-2630/aa7cb5>.
116. He, L., Zhang, W. X. & Zhang, X. D. Topological all-optical logic gates based on two-dimensional photonic crystals. *Opt. Express* **27**, 25841–25859 (2019). <https://doi.org/10.1364/OE.27.025841>.
117. Merlo, J. M., Wu, X., Kempa, K. & Naughton, M. J. All-optical logic gates based on anomalous Floquet photonic topological insulator structures. *J. Opt.* **23**, 065001 (2021). <https://doi.org/10.1088/2040-8986/abf8cd>.
118. Xu, X., Zhang, H., Huang, J., Zhai, N. & Liu, Y. Logic gate and optical half-adder designed by photonic crystal based on BPSK signals. *Optik* **259**, 168984 (2022). <https://doi.org/10.1016/j.ijleo.2022.168984>.
119. Barik, S. et al. A topological quantum optics interface. *Science* **359**, 666–668 (2018). <https://doi.org/10.1126/science.aag0327>.
120. Blanco-Redondo, A., Bell, B., Oren, D., Eggleton, B. J. & Segev, M. Topological protection of biphoton states. *Science* **362**, 568–571 (2018). <https://doi.org/10.1126/science.aau4296>.
121. Wang, M. et al. Topologically protected entangled photonic states. *Nanophotonics* **8**, 1327–1335 (2019). <https://doi.org/10.1515/nanoph-2019-0058>.
122. Doyle, C. et al. Biphoton entanglement of topologically distinct modes. *Phys. Rev. A* **105**, 023513 (2022). <https://doi.org/10.1103/PhysRevA.105.023513>.
123. Wang, Y. et al. Topological protection of two-photon quantum correlation on a photonic chip. *Optica* **6**, 955–960 (2019). <https://doi.org/10.1364/OPTICA.6.000955>.
124. Wang, Y. et al. Topologically protected polarization quantum entanglement on a photonic chip. *Chip* **1**, 100003 (2022). <https://doi.org/10.1016/j.chip.2022.100003>.
125. Tambasco, J.-L. et al. Quantum interference of topological states of light. *Sci. Adv.* **4**, eaat3187 (2018). <https://doi.org/10.1126/sciadv.aat3187>.
126. Ren, R.-J. et al. Topologically protecting squeezed light on a photonic chip. *Photonics Res.* **10**, 456–464 (2022). <https://doi.org/10.1364/PRJ.445728>.
127. Chen, Y. et al. Topologically protected valley-dependent quantum photonic circuits. *Phys. Rev. Lett.* **126**, 230503 (2021). <https://doi.org/10.1103/PhysRevLett.126.230503>.
128. Porras, D. & Fernández-Lorenzo, S. Topological amplification in photonic lattices. *Phys. Rev. Lett.* **122**, 143901 (2019). <https://doi.org/10.1103/PhysRevLett.122.143901>.
129. Bhattacharjee, S., Biswas, P. & Ghosh, S. Identifying topological signature of 1D photonic lattice by Zak phase analysis and towards robust amplification of edge state. *J. Opt.* **23**, 095604 (2021). <https://doi.org/10.1088/2040-8986/ac11ab>.
130. Ling, H. Y. & Kain, B. Selection rule for topological amplifiers in Bogoliubov-de Gennes systems. *Phys. Rev. A* **104**, 013305 (2021). <https://doi.org/10.1103/PhysRevA.104.013305>.
131. Galilo, B., Lee, D. K. K. & Barnett, R. Selective population of edge states in a 2D topological band system. *Phys. Rev. Lett.* **115**, 245302 (2015). <https://doi.org/10.1103/PhysRevLett.115.245302>.
132. Elshahat, S., Abood, I., Liang, Z., Pei, J. & Ouyang, Z. Elongated-hexagonal photonic crystal for buffering, sensing, and modulation. *Nanomaterials* **11**, 809 (2021). <https://doi.org/10.3390/nano11030809>.
133. Elshahat, S., Abood, I., Esmail, M. S. M., Ouyang, Z. & Lu, C. One-dimensional topological photonic crystal mirror heterostructure for sensing. *Nanomaterials* **11**, 1940 (2021). <https://doi.org/10.3390/nano11081940>.
134. Elshahat, S., Mohamed, Z. E. A., Almkhtar, M. & Lu, C. High tunability and sensitivity of 1D topological photonic crystal heterostructure. *J. Opt.* **24**, 035004 (2022). <https://doi.org/10.1088/2040-8986/ac45d2>.
135. Kunst, F. K., Edvardsson, E., Budich, J. C. & Bergholtz, E. J. Biorthogonal bulk-boundary correspondence in non-Hermitian systems. *Phys. Rev. Lett.* **121**, 026808 (2018). <https://doi.org/10.1103/PhysRevLett.121.026808>.
136. Weidemann, S. et al. Topological funneling of light. *Science* **368**, 311–314 (2020). <https://doi.org/10.1126/science.aaz8727>.
137. Budich, J. C. & Bergholtz, E. J. Non-Hermitian topological sensors. *Phys. Rev. Lett.* **125**, 180403 (2020). <https://doi.org/10.1103/PhysRevLett.125.180403>.
138. Gong, Z. et al. Topological phases of non-Hermitian systems. *Phys. Rev. X* **8**, 031079 (2018). <https://doi.org/10.1103/PhysRevX.8.031079>.
139. Koch, R. & Budich, J. C. Bulk-boundary correspondence in non-Hermitian systems: stability analysis for generalized boundary conditions. *Eur. Phys. J. D* **74**, 70 (2020). <https://doi.org/10.1140/epjd/e2020-100641-y>.
140. Koch, F. & Budich, J. C. Quantum non-Hermitian topological sensors. *Phys. Rev. Res.* **4**, 013113 (2022). <https://doi.org/10.1103/PhysRevResearch.4.013113>.
141. Wu, X. et al. Topological corner modes induced by Dirac vortices in arbitrary geometry. *Phys. Rev. Lett.* **126**, 226802 (2021). <https://doi.org/10.1103/PhysRevLett.126.226802>.
142. Zhao, H. et al. Non-Hermitian topological light steering. *Science* **365**, 1163–1166 (2019). <https://doi.org/10.1126/science.aay1064>.
143. Zhong, J. et al. Nontrivial point-gap topology and non-Hermitian skin effect in photonic crystals. *Phys. Rev. B* **104**, 125416 (2021). <https://doi.org/10.1103/PhysRevB.104.125416>.
144. Yang, C.-N. & Mills, R. L. Conservation of isotopic spin and isotopic gauge invariance. *Phys. Rev.* **96**, 191 (1954). <https://doi.org/10.1103/PhysRev.96.191>.
145. Wu, T. T. & Yang, C. N. Concept of nonintegrable phase factors and global formulation of gauge fields. *Phys. Rev. D* **12**, 3845 (1975). <https://doi.org/10.1103/PhysRevD.12.3845>.
146. Iadecola, T., Schuster, T. & Chamon, C. Non-abelian braiding of light. *Phys. Rev. Lett.* **117**, 073901 (2016). <https://doi.org/10.1103/PhysRevLett.117.073901>.

147. Zhao, Y., Liu, X.-X. & Alù, A. Recent advances on optical metasurfaces. *J. Opt.* **16**, 123001 (2014). <https://doi.org/10.1088/2040-8978/16/12/123001>.
148. Lv, H., Bai, Y., Yao, J. & Yang, Y. Generation of optical vortices using the metasurface combining dynamic and geometric phases, In *10th International Symposium on Advanced Optical Manufacturing and Testing Technologies: Micro-and Nano-Optics, Catenary Optics, and Subwavelength Electromagnetics* **12072**, 26–32 (2021). <https://doi.org/10.1117/12.2604457>.
149. Zhang, Z., Yang, J., Du, T. & Jiang, X. Topological multipolar corner state in a supercell metasurface and its interplay with two-dimensional materials. *Photonics Res.* **10**, 855–869 (2022). <https://doi.org/10.1364/PRJ.443025>.
150. Li, M. et al. Experimental observation of topological Z2 exciton-polaritons in transition metal dichalcogenide monolayers. *Nat. Commun.* **12**, 1–10 (2021). <https://doi.org/10.1038/s41467-021-24728-y>.
151. Liu, W. et al. Generation of helical topological exciton-polaritons. *Science* **370**, 600–604 (2020). <https://doi.org/10.1126/science.abc4975>.
152. Gorlach, M. A. et al. Far-field probing of leaky topological states in all-dielectric metasurfaces. *Nat. Commun.* **9**, 1–8 (2018). <https://doi.org/10.1038/s41467-018-03330-9>.
153. Smirnova, D. et al. Third-harmonic generation in photonic topological metasurfaces. *Phys. Rev. Lett.* **123**, 103901 (2019). <https://doi.org/10.1103/PhysRevLett.123.103901>.
154. Liu, Z. et al. Integrated nanophotonic wavelength router based on an intelligent algorithm. *Optica* **6**, 1367–1373 (2019). <https://doi.org/10.1364/OPTICA.6.001367>.
155. Lu, C. et al. Nanophotonic polarization routers based on an intelligent algorithm. *Adv. Opt. Mater.* **8**, 1902018 (2020). <https://doi.org/10.1002/adom.201902018>.
156. Christiansen, R. E., Wang, F., Sigmund, O. & Stobbe, S. Designing photonic topological insulators with quantum-spin-Hall edge states using topology optimization. *Nanophotonics* **8**, 1363–1369 (2019). <https://doi.org/10.1515/nanoph-2019-0057>.
157. Chen, Y., Meng, F., Kivshar, Y., Jia, B. & Huang, X. Inverse design of higher-order photonic topological insulators. *Phys. Rev. Res.* **2**, 023115 (2020). <https://doi.org/10.1103/PhysRevResearch.2.023115>.
158. Chen, Y., Meng, F., Zhu, J. & Huang, X. Inverse design of second-order photonic topological insulators in C3-symmetric lattices. *Appl. Math. Model.* **102**, 194–206 (2022). <https://doi.org/10.1016/j.apm.2021.09.039>.
159. Ma, L. et al. Intelligent algorithms: new avenues for designing nanophotonic devices [Invited]. *Chin. Opt. Lett.* **19**, 011301 (2021). <https://doi.org/10.3788/COL202119.011301>.

## MISCELLANEA

**Acknowledgements** This work is supported by National Natural Science Foundation of China (12274031, 92050110, 12275145); Beijing Institute of Technology Research Fund Program for Teli Young Fellows. The authors thank Dr. Xinyue Wang for inputs in subsection 8.3.

**Declaration of Competing Interest** The authors declare no competing interests.

© 2022 The Authors. Published by Elsevier B.V. on behalf of Shanghai Jiao Tong University. This is an open access article under the CC BY license (<http://creativecommons.org/licenses/by/4.0/>)